Old Dominion University

ODU Digital Commons

Mechanical & Aerospace Engineering Theses & Dissertations

Mechanical & Aerospace Engineering

Spring 2008

Process Study for the Design of Small-Scale 2 Kelvin Refrigeration Systems

Peter N. Knudsen
Old Dominion University, knudsen@frib.msu.edu

Follow this and additional works at: https://digitalcommons.odu.edu/mae_etds

 Part of the Heat Transfer, Combustion Commons

Recommended Citation

Knudsen, Peter N.. "Process Study for the Design of Small-Scale 2 Kelvin Refrigeration Systems" (2008). Master of Science (MS), Thesis, Mechanical & Aerospace Engineering, Old Dominion University, DOI: 10.25777/2S45-TV78
https://digitalcommons.odu.edu/mae_etds/47

This Thesis is brought to you for free and open access by the Mechanical & Aerospace Engineering at ODU Digital Commons. It has been accepted for inclusion in Mechanical & Aerospace Engineering Theses & Dissertations by an authorized administrator of ODU Digital Commons. For more information, please contact digitalcommons@odu.edu.

PROCESS STUDY FOR THE DESIGN OF SMALL SCALE 2 KELVIN REFRIGERATION SYSTEMS

By

Peter N. Knudsen
B.S., Mechanical Engineering, December 1990, Colorado State University

A Thesis Submitted to the Faculty of
Old Dominion University in Partial Fulfillment of the
Requirement for the Degree of

MASTER OF SCIENCE

MECHANICAL ENGINEERING

OLD DOMINION UNIVERSITY
May 2008

Approved by:

_____
Ayodeji O. Demuren (Director)

_____
Sushil K. Chaturvedi (Member)

_____
Venkatarao Ganni (Member)

ABSTRACT

PROCESS STUDY FOR THE DESIGN OF SMALL SCALE
2 KELVIN REFRIGERATION SYSTEMS

Peter N. Knudsen
Old Dominion University, 2008
Director: Dr. Ayodeji O. Demuren

Helium refrigeration at temperatures below 4.5-Kelvin (K), but greater than 0.8-K typically employ a sub-atmospheric process utilizing a vacuum pumping system. These types of helium refrigerators are of keen interest to present and future particle physics programs utilizing super-conducting magnet or radio-frequency technology. As such, there is a need for small scale 2-K helium refrigeration systems (i.e., those that operated below the lambda temperature) in small laboratories and test facilities at this time. This study establishes the key process parameter choices of flow ratio, heat-exchanger size, and supply pressure, and how they influence the overall system performance for various process configurations that do not utilize rotating machinery within the cold box (i.e., turbo-machinery for either cryogenic vacuum pumping or expansion) but do utilize a separate commercially available 4.5-K helium liquefier system. Three 2-K process configurations are studied to determine the key process parameter values that yield the best performance. These process configurations are compared to the commonly employed (but inefficient) direct vacuum pumping process, which typically uses a dewar as the 4.5-K liquid helium supply source. It is found that the performance of these configurations is similar and substantially superior to direct vacuum pumping, providing an inverse coefficient of performance of around 1800 W/W.

Copyright © 2008 Peter N. Knudsen. All Rights Reserved.

To my wife Bonni and my children Brad and Elizabeth,
for their love and support,
and
to Christ Jesus,
for His grace and His perfect unconditional love
which He made manifest and secured at the Cross of Calvary

Colossians 1:15-23

In memory of Marie Arenius

ACKNOWLEDGMENTS

In walking through a library I am at first amazed by the accumulated knowledge stored on the shelves, then ponder the undocumented knowledge that has likely been lost over the millennia and then wonder a bit at the inevitable demise of the minute quantity of imperfectly understood knowledge in my possession. It is certain that this work has not added to the Creator's knowledge or deepened His understanding! Perhaps it will add to the knowledge and/or deepen the understanding of the created. Ultimately though, it seems that its lasting value is mostly for the author. It is fitting then that my acknowledgement is not just of the shared provision of common Grace so kindly given, but that He actually cares about such a small thing as this work, and even more so, the condition of my soul at its completion. An acknowledgement to Him seems so trite, but I am compelled to give it.

I am grateful to my wife who has always humbly interceded on my behalf, including this thesis.

I also want to acknowledge by mentor Rao Ganni, who is the most intuitive, practical and capable engineer I have ever met. Under his guidance and tutelage I have learned everything of importance in this field: details, concepts and methodology. He loves excellence, pursues understanding, propels himself and everyone willing to come along at break-neck speed but knows when it's time to get it done and to be done…for now. I've learned much by watching his ability to encourage others in their strengths and harness those strengths for the common good of all. I am also very grateful for his patience.

In addition, I would like acknowledge the members of the Jefferson Lab cryogenics group whose dedication to excellence and hard work make it an honor to be counted as their colleague.

I would be remiss not to thank James Fesmire, my friend, who introduced me to this business of cryogenics with indelible enthusiasm. After fourteen years it has not worn off.

Finally I want to acknowledge and express thanks to my advisor, Professor Ayodeji Demuren, for his direction and guidance on this thesis.

TABLE OF CONTENTS

TABLE OF CONTENTS

LIST OF TABLES

LIST OF FIGURES

LIST OF FIGURES

NOMENCLATURE

ADL	Arthur D. Little
C_p	specific heat at constant pressure
COP_{INV}	inverse coefficient of performance
CTF	cryogenics test facility
DESY	Deutsches Elektronen-Synchrotron
h	enthalpy (per unit mass)
HP	high pressure
HX	heat exchanger
JLab	Jefferson Lab
JT	Joule-Thompson
LMTD	log-mean temperature difference
LN	liquid nitrogen
LP	low pressure
NTU or Ntu	number of (heat exchanger) heat transfer units
$p_{h,1}$	supply pressure to 2-K cold box
$p_{r,c}$	compressor pressure ratio
ppm	parts-per-million
RSC	rotary screw compressor
s	entropy (per unit mass)
T_0	reference temperature (at zero availability)
TTF	TESLA test facility

NOMENCLATURE

UA	net thermal rating
VAP	ambient air vaporizer (or heat exchanger)
VPS	vacuum pumping system
Δp_{ℓ}	sub-atmospheric stream pressure drop
ε	exergy (per unit mass)
η_C	Carnot efficiency
η_{iso} or η_i	isothermal efficiency
ξ_{hl}	flow ratio (or flow imbalance)

1. INTRODUCTION

1.1 Purpose of Study

The normal boiling point (at 1 atmosphere, or 'atm') for helium is 4.22 Kelvin (K). As such a cryogenic process using helium that operates below this temperature requires the condition of sub-atmospheric pressures (known in the field as processes below 4.5 K). There are four methods typically used for providing refrigeration at temperatures below 4.5 K, but above 0.8 K. They are direct vacuum pumping (i.e., wasting the sensible refrigeration available from the load to ambient temperature; no refrigeration recovery), and refrigeration recovery using either warm vacuum pumps, cryogenic centrifugal turbo-compressors (known in the field as 'cold compressors') or a combination of both warm vacuum pumps and cold compressors. The term 'refrigeration recovery' (as it is known in the field) means the attempt to utilize the sensible heat of the sub-atmospheric helium boil-off, resulting from the heat load, to improve the process's efficiency. In practice this requires the use of heat exchangers to reduce the load feed stream temperature (enthalpy) by utilizing the refrigeration from the sub-atmospheric helium boil-off stream. For most common presently known applications, the technologies that require sub-atmospheric helium pressures operate at saturation temperatures of 1.8 to 2.2 K. All of these shall be referred to as 2-K processes or 2-K systems.

The study's intended end objective is to provide a process design basis for a 'small' 2-K refrigeration recovery unit (also referred to as a '2-K cold box') working in conjunction with a *commercially available*

(1) 4.5-K helium liquefaction system (also referred to as the ‘4.5-K plant’) [1, 2]. This liquefier system includes its own compression and gas management system.

(2) Helium vacuum pumping system.

(3) Helium compression system.

By ‘small’ it is meant nominal 2-K loads on the order of 100 Watts (W); i.e., requiring 4.5-K make-up mass flows from the liquefier system in the approximate magnitude of a couple of grams per second (i.e., about 2 g/s). This study does not address processes using cold compression, as these are typically used on medium to larger systems [3, 4]. As such, there is no rotating machinery within the (envisioned) 2-K cold box; although the commercially available 4.5-K liquefaction system most certainly does employ rotating machinery (i.e., compressors and expanders). The 2-K cold box in this study is intended only to utilize passive components such as heat exchangers and throttling valves.

1.2 Study Goals

(1) Identify possible 2-K process configurations utilizing the major sub-systems mentioned (i.e., 2-K cold box, 4.5-K liquefier system, vacuum pumping system and compression system).

(2) Establish the key process parameter choices for the selected process configurations.

(3) Characterize the influence of the key process parameter choices on the overall 2-K system performance.

1.3 Literature Review

Sam Collins at Arthur D. Little (ADL) made a test refrigerator in cir. 1967 that operated at 1.8 K and 30 W, used a commercial Collins-ADL helium liquefier (supplying to a 2-K cold box) and commercial vacuum pumps [5, 6]. Rather than a helium supply at 3 atm and 4.5 K more typical from present day helium liquefiers, the commercial Collins-ADL liquefier supplied helium at 15 atm and 7.0 K to the 2-K cold box. There are a number of 2-K systems that supported heat loads on the order of 100 W, but had the 4.5-K liquefier and 2-K cold box conjoined [7-11] and others that used cold compressors [12-16].

However, to the author's knowledge, from a literature review and discussions with those who have worked in the field for the past 35 years, the following can be stated:

(1) No systematic process study was found identifying the key parameters and their influence on the performance of such 2-K systems of the type proposed to be studied.

(2) It appears that there have been two 2-K systems built that are similar to the type proposed to be studied. These are the Cryogenics Test Facility (CTF) at Jefferson Lab (JLab) and the TESLA test facility (TTF) at Deutsches Elektronen-Synchrotron (DESY) [17, 18]. The author was not able to confirm whether the TTF at DESY is still operating, or obtain performance data. However, although at 14 years beyond its original end of use date, the CTF at JLab has been operating since 1989. Both of these systems support a 2-K heat load on the order of 100 W, have a distinctly separate commercial 4.5-K helium liquefier (supplying super-critical

helium to the 2-K cold box) and do not use cold compressors. Refer to TABLE 1.2.1 for a brief comparison summary.

TABLE 1.2.1 – Similar 2-K Systems

	JLab CTF	**DESY TTF**
Load Temperature	2.0 K	1.8 K
Heat Load	180 W (9 g/s)	200 W (10 g/s)
4.5-K Plant	Koch Model 2200	Linde AG 900 W at 4.5 K 2 kW at 70 K
Vacuum Pumps	Kinney Lobe Blower, KMBD-8000 Kinney Liquid Ring Pump, KLRC-2100S	Leybold Lobe Blowers RA16000, RA13000, RA9001 Leybold Rotary Vane Pumps, SV1200

2. THEORY & CHARACTERIZATIONS

2.1 Process Study Optimization Goal

Before undertaking a process study, it must be decided whether the primary optimization is for maximum overall efficiency or maximum system (load) capacity. The latter is typically (but not always) the optimization objective when dealing with existing equipment, and the user is interested in obtaining the most capacity from what is installed. The former seeks to minimize input power and utility consumption for a specified load and is more typically (but not always) of interest for new designs when equipment is to be either fabricated and/or selected from a range of choices. Although there are other optimization goals for process design like maximum reliability, maximum availability and minimum maintenance, these are strongly influenced by specific project requirements such as end user needs, available project capital and funding allocations between operating and capital costs. It is important to understand that these optimizations are not mutually exclusive. Usually the process optimization of maximum overall efficiency results in the optimum condition (i.e., a global optimization). If this is not the case, the process paths and/or process control philosophies should be re-evaluated to understand the reasons.

Therefore, in this study we will seek to maximize the overall efficiency using typical realistic equipment performance that is not specific to any one manufacturer.

2.2 Process Parameters

The process parameters for this study can be divided into two broad categories. The first category is those parameters that are at either constant values or have a fixed characterization. The second category is those parameters that are varied either over some pre-determined range or set of proposed configurations. These categories may be referred to as ‘fixed’ parameters and ‘varied’ parameters, respectively. The varied parameters are proposed to be the key process parameters to characterize the overall performance of the 2-K system, as considered by this study.

2.2.1 Fixed Process Parameters

The overall efficiency of a 2-K system, of the type proposed to be studied, is strongly influenced by the following:

(1) The precise load temperature. For this study a load temperature (in the helium II bath) of 2.0 K, corresponding to a saturation pressure of 0.0310 atm, will be assumed. FIGURE 2.2.1 shows that the saturation pressure of helium is logarithmic with respect the temperature. So, a linear change in temperature corresponds to an exponential change in pressure, which corresponds to a linear change in isothermal input power.

(2) Overall Carnot efficiency of the commercial 4.5-K liquefier system includes not only the cold box but also its compression and gas management system. For this study a constant value, specific to the particular process configuration and capacity, will be assumed. The overall Carnot efficiency, which is the load exergy (or reversible power) per total input power, can vary considerably with the liquefier capacity

[19]. APPENDIX A shows recent unpublished data compiled by the author for selected 4.5-K plant efficiencies.

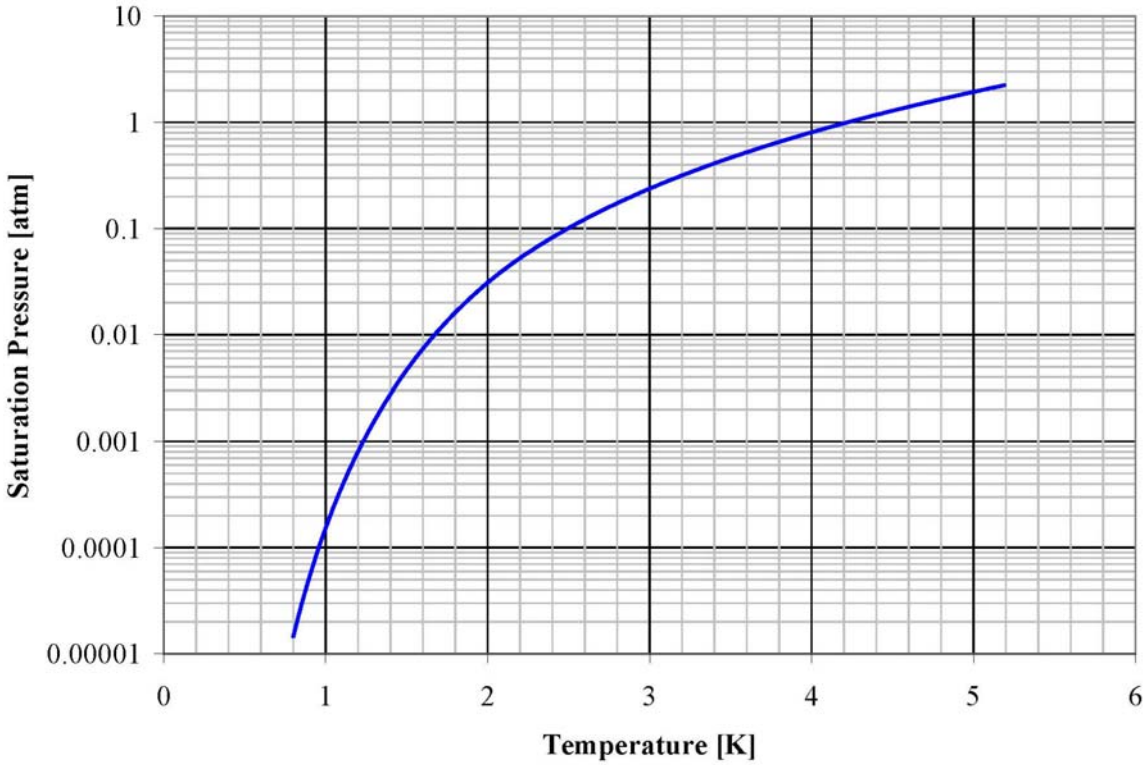

FIGURE 2.2.1 – Helium Saturation Pressure vs. Temperature

(3) Isothermal efficiency of the 2-K system compressor(s). For this study a fixed characterization based upon the compressor (discharge to suction) pressure ratio will be used. It is known that the pressure ratio is the primary independent variable for the isothermal and volumetric efficiency of oil-flooded rotary screw compressors [20]. Although the 2-K system compressors may be similar in type and/or size to the compression system (included in and) used by the 4.5-K helium liquefier system, they are *not* the same equipment.

(4) Isothermal efficiency of the vacuum pump system. For this study a constant value will be assumed, because the (discharge to suction) pressure ratio across the vacuum pumping system remains almost the same for all cases. The input power to the vacuum pumping system typically comprises (at least) 40 percent (%) of the total input power and total exergy losses for 2-K systems using refrigeration recovery.

(5) Parasitic (non-load) heat in-leak into the process streams and components from radiation and support/piping conduction. For this study a constant value of 55 W will be assumed. The distribution of this heat in-leak is also important and has been divided (proportionally) according to the heat exchanger size. This heat in-leak may be somewhat large, but it will also deter from a too optimistic performance projection.

(6) Sub-atmospheric stream pressure drop from the load to the suction of the vacuum pumping system. For this study a fixed characterization based upon the total sub-atmospheric stream heat exchanger NTU's (as commonly referred to in engineering) will be assumed. Pressure drop is proportional to flow length, and the heat exchanger NTU's are roughly proportional to the same. It is easily verified that the ratio of pressure drop to stream pressure is proportional to the irreversibility and exergetic loss. However, more importantly, as the pressure drop increases the vacuum pumping system capacity to handle the sub-atmospheric flow from the 2-K load (proportionally) decreases. As they should, past

designs have concerned themselves greatly with the heat exchanger designs for a minimal pressure loss in the sub-atmospheric stream.

2.2.2 Varied Process Parameters

As with the fixed process parameters mentioned, the overall efficiency of a 2.0-K system, as considered by this study, is also strongly influenced by the following:

(1) Ratio of high pressure helium flow to sub-atmospheric helium flow in the main heat exchanger; also referred to as the 'flow imbalance' or 'flow ratio'. This will be ranged from 40 to 100%, as the solution allows.

(2) Total heat exchanger NTU's. This will be ranged from 20 to 45 NTU's at 5 NTU increments. The NTU's for a heat exchanger roughly correspond to its effective length and the net thermal rating (also known as the 'UA') to its volume. Since the overall process is fixed between ambient and the load temperatures, and the sub-atmospheric return flow is fixed, the heat exchanger cross-sectional area is roughly fixed. So, for this study, the total NTU's will be proportional to the total UA, which is the heat exchanger size. Therefore, it is the sum total heat exchanger size that is being varied. Total heat exchanger NTU's greater than 45 were not studied due to the resulting excessive sub-atmospheric stream pressure drop.

(3) Supply pressure to the 2-K cold box, from the compressor discharge. This will be ranged from 6 to 18 atm, at 3 atm increments. This determines the availability (i.e., exergy) supplied to the 2-K cold box and to some degree the input required for the compressor(s).

2.3 Helium's Specific Heat Capacity and Heat Exchangers

FIGURE 2.3.1 shows the specific heat (at constant pressure, labeled C_p, with units of Joules per gram per Kelvin, or J/g-K) for helium at selected pressures (labeled p). As is well known from basic thermodynamics, the non-constancy of the specific heat is due to presence of the liquid-vapor 'dome' where the fluid 'must impose the work of the latent heat on itself' to keep the super-critical fluid enthalpy close to the liquid enthalpy at the same temperature. This effect is most important and pronounced near the critical pressure (for helium, 2.245 atm) and tapers off quickly as the pressure increases. This real fluid effect is quite beneficial, in that we can keep a load at a constant temperature by boiling off the liquid. However, the variation in specific heat introduces additional heat exchanger irreversibility (that would not otherwise be present if it were an ideal gas). So, a significant process design challenge is to deal with this specific heat variation in the most reversible manner possible. As has been known for some time, the most reversible temperature difference distribution for a counter-flow heat exchanger with an ideal gas is a linear distribution [21]. This is considerably different from the logarithmic temperature distribution predicted using a constant overall heat transfer coefficient. So, at the outset it would seem the challenge is quite difficult even theoretically. However, in practice the exergetic loss due to the heat exchangers in the 2-K cold box (including the ambient air vaporizer) should only be in the order of 5% of the total input power. To deal with the irreversibility due to a finite temperature difference in the heat exchangers, the length can be increased. So, of the 5% total input power loss due to heat exchanger irreversibilities (mentioned above), about 13% (i.e., less than 1% of the input power) is due to the pressure loss, and of this (13%) about 98% (i.e., less than 1% of the input power) is due

to the sub-atmospheric stream pressure loss. So, the sub-atmospheric pressure loss is essentially the source of all the heat exchanger exergetic loss due to pressure, but it is small. As long as the heat exchangers are sufficiently long (i.e., at least 1 meter for every 10 NTU's for brazed-aluminum heat exchangers; [3]) and have adequate cross-sectional area for the sub-atmospheric stream (so that pressure loss is limited to no more than 25% of the load saturation pressure, due to available practical equipment limitations), the problems of variation of specific heat cause more theoretical consternation than is practically warranted.

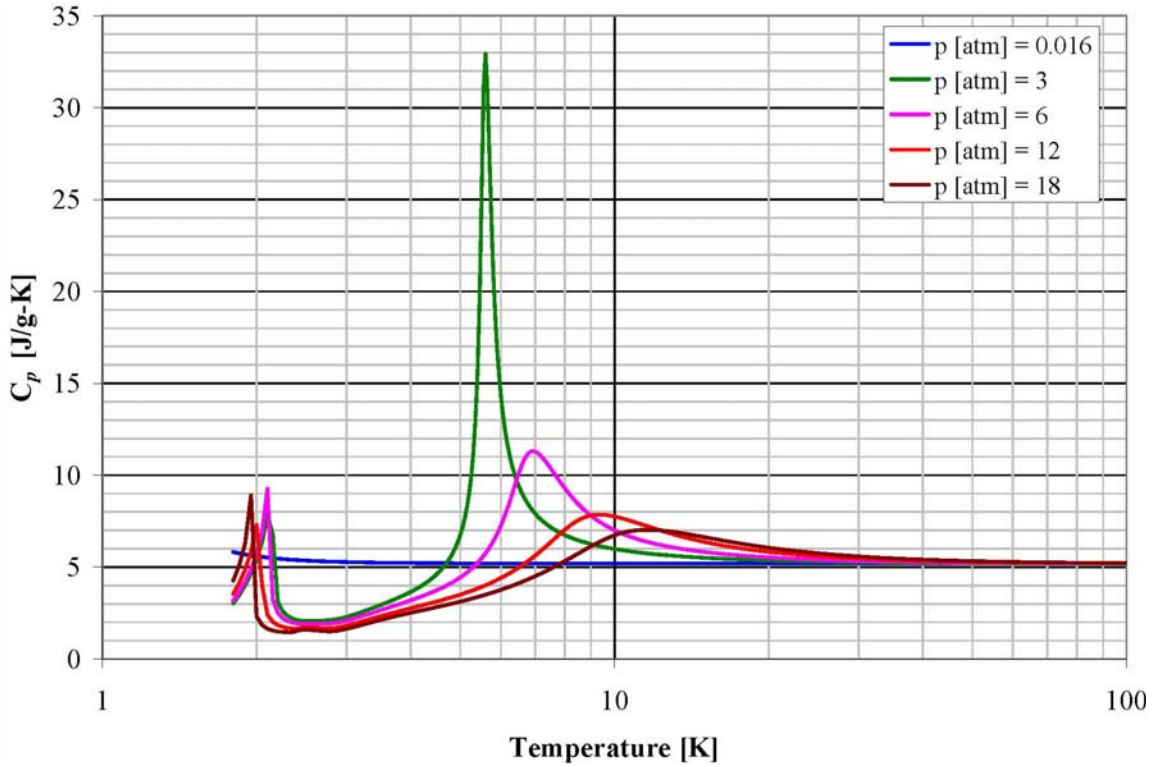

FIGURE 2.3.1 – Helium Specific Heat at Selected Pressures

However, in general there is a considerable optimization trade-off between the heat exchanger length and cross-sectional area with respect to the overall effect on the process, due to the resulting heat exchanger pressure drop and (thermal) effectiveness. That is, for a fixed cross-sectional area, as the heat exchanger length is increased, the

irreversibility due to pressure drop will increase, but the irreversibility due to the temperature difference will decrease (as the heat transfer area increases). The same is true for a fixed length, as the heat exchanger cross-sectional area is decreased (since the Reynold's number and consequently the Colburn '*j*' factor increases [22]). The problem becomes process type-(e.g., 4.5-K liquefier, 2-K refrigerator) and equipment type-(e.g., brazed aluminum or spiral-wound finned heat exchangers) specific. That is, to the overall process performance trade-off between the heat exchanger usage of the high pressure stream availability and minimizing the heat exchanger low pressure stream pressure loss (to not exceed some practical limit) vs. the increase in thermal performance (with a longer and/or small cross-section heat exchanger). However, this topic is a treatise of its own.

2.4 Model Component Characterizations

2.4.1 Fluid Properties

All fluid properties were evaluated using the commercially available code 'HePak' (version 3.4) for helium properties and 'GasPak' (version 3.30) for nitrogen properties. HePak can be used down to 0.8 K and includes helium II (super-fluid) thermodynamic and transport properties. The real fluid properties were used in every calculation for both helium and nitrogen.

2.4.2 4.5-K Helium Liquefaction System

For large 4.5-K helium liquefiers (greater than about 50 g/s) the Carnot efficiency can be about 25% for a well match compressor system. However, for 4.5-K plants

considered by this study, providing 2 to 3 g/s of liquefaction capacity, the Carnot efficiency is around 10% (see APPENDIX A). As is usual of modern 4.5-K helium liquefiers the supply (from the liquefier) has been assumed to be 3 atm and 4.5 K. This is super-critical fluid which is close to the liquid enthalpy for ease of flow distribution.

2.4.3 Vacuum Pumping System

An isothermal efficiency of 14.5% for the vacuum pumping system, comprised of a liquid-ring pump [23] and a lobe (roots)-blower [24], is based upon unpublished data from JLab's CTF vacuum pumping system (see APPENDIX B). This value is considered to be realistic (i.e., not too optimistic, but also not very conservative).

2.4.4 Rotary Screw Compressor(s)

The isothermal efficiency of the oil-flooded rotary screw compressor(s) was taken from published data [20] and unpublished data [25] from testing of small hermetically sealed oil-flooded rotary screw compressors (refer to APPENDIX C). A linear characterization of the isothermal efficiency vs. compressor pressure ratio was used (which is a good approximation in the range of this study's interest) as shown below:

$$\eta_{iso} = 0.6 - 0.0177*(p_{r,c} - 3) \qquad (2.4\text{-}1)$$

With $p_{r,c}$ the ratio of discharge to suction pressure (i.e., compressor pressure ratio). This characterization is valid for compressor pressure ratios between 3 and 18.

2.4.5 Heat Exchangers

A linear characterization of the pressure drop of the sub-atmospheric stream vs. heat exchanger NTU's was used as shown below:

$$\Delta p_{\ell}\,[\text{atm}] = (2.03x10^{-4})*\text{NTU} \qquad (2.4\text{-}2)$$

With ‘NTU’ being the NTU for each heat exchanger considered. Since the total NTU’s ranged from 20 to 45 (in increments of 5), this also establishes the maximum sub-atmospheric stream pressure drop for each total NTU case.

For the heat exchanger analysis, the integrated cooling curves were calculated. A typical log-mean-temperature-difference (LMTD) analysis, assuming constant heat capacity rates, is not valid since the specific heat for helium can vary considerably below 20 K. To calculate the heat exchanger UA and NTU’s for varying specific heat, the methodology is to divide the heat exchanger into smaller sub-sections where the constant stream capacity assumption can be imposed as an average over the sub-section [26]. The calculation of the heat exchanger effectiveness is somewhat more involved. This is due to the fact that, unlike a fluid idealized with a constant specific heat, the temperature pinch (i..e., the minimum temperature difference between streams) may not occur on the warm or cold end. In fact, below 20 K, often the temperature pinch will occur at some location between the heat exchanger ends. So, an iterative procedure is required to find the pinch point of a given heat exchanger. The condition where the stream temperature difference at the pinch point is zero is the maximum possible duty (for the given inlet process conditions, stream pressure drop and heat in-leak).

2.5 Exergy and Exergy Usage

Exergy analysis [27], or availability analysis as it is sometimes called, is an extremely useful method for a consistent determination of the minimum required work (i.e., the reversible work) for a process, based solely on the process intensive thermodynamic properties. The process may be any thermodynamic process, steady, un-

steady, single fluid, multi-phase or chemical. Using this method, the expenditure of the input power to its intended (useful) purpose(s) and non-useful process component losses may be studied. For a study like this, such analysis is very useful in comparing losses of similar components used under different process conditions and configurations, as well as, identifying the major component loss contributors needing further study and/or technological innovation.

Physical exergy is defined as follows:

$$\varepsilon = h - T_0 * s \qquad (2.5)$$

With 'h' the enthalpy, 'T_0' the absolute reference temperature and 's' the entropy. The reference temperature, T_0, is the absolute temperature for which there is zero availability. Although, typically taken at 300 K, for cases where the process availability is provided by rotating machinery cooled by water whose heat is removed by evaporative cooling, the reference temperature is more precisely the environmental wet bulb temperature. It should also be noted that exergy has the same units as energy.

2.6 Measures of Process Performance

There are many constructs used to evaluate and compare process performance. The crucial elements in any construct are its clear definition and an adherence by the process engineer in its implementation. The Carnot efficiency (η_C), and inverse coefficient of performance (COP_{INV}) are such constructs.

For this study, the Carnot efficiency is the ratio of the availability (i.e., the exergy flux for a steady state process) provided to the 'load' to the total input power required by

the process. The availability to the load is also sometimes known in the field as the ‘load Carnot power’.

The 2-K system ‘load’ interface is defined by the study to be between the 2-K cold box and sub-atmospheric helium II bath. The supply interface to the load is two-phase at the bath pressure and saturation temperature, and the return interface from the load is single-phase saturated vapor. The study assumes a steady bath pressure, no mass accumulation and that all heat (electrical, radio-frequency loss generated, etc.) into the bath goes into boiling-off the liquid (rather than super-heating the vapor). The total input power is the total equivalent electrical power supplied to the process.

For cases involving liquid nitrogen (LN) pre-cooling, the LN is an input utility (like the electrical power) used to ‘pre-cool’ the make-up helium from ambient temperature down to approximately 80 K. Some portion of the supplied LN is necessary for heat exchanger losses. These losses are primarily due to finite stream temperature differences, but are also due to non-constant stream capacity (i.e., real fluid effects) and heat in-leak. This utility provides supplemental refrigeration to what would otherwise have to be accomplished using additional helium flow that is compressed and expanded. The methodology to find the equivalent electrical input power is to take availability given by the LN pre-cooling and divide by an efficiency, known as the LN pre-cooling Carnot efficiency. For this study, the LN pre-cooling Carnot efficiency is taken as 35%, as is typical for this application.

Consistency of the interface locations and process conditions between the 4.5-K plant and 2-K system is important so that comparing performance parameters is meaningful. For example, as in [5, 6], consider the case of the 2-K cold box supplying a

portion of its high pressure stream to the 4.5-K liquefier, to provide additional work extraction (e.g., say it is combined with other flow supplied to an expander) and refrigeration. Even though this may be very beneficial to the overall process efficiency, in such a case the commercial liquefier is no longer a standard model. This increases the total system cost considerably, since it requires re-engineering and introduces additional performance risks. Also, it would become necessary to model several commercial 4.5-K liquefiers to properly evaluate the effect of the modifications on the 2-K system in overall performance and efficiency. With the wide range of varied parameters being examined for this study, the kind of information that would be required of the manufacturers is considered proprietary (e.g., compressor and turbine - flow and efficiency characterizations, heat exchanger sizes, and heat in-leaks). Even if all this was done, the results may be invalidated as a manufacturer makes its own improvements and modifications to its commercial designs. Therefore, since the optimization becomes manufacturer specific, this approach has been avoided.

There are two (depending on the model configuration studied) interface locations between the 4.5-K liquefier and 2-K systems. The first, as previously mentioned, is the helium supply at 3 atm and 4.5 K from the 4.5-K liquefier to the 2-K cold box. The second is, depending on the model configuration studied, either a helium stream at 1.05 atm and 300 K from the 2-K system (i.e., a fraction of the flow from the vacuum pumping system discharge) to the 4.5-K liquefier system, or a helium stream at 1.2 atm and 79.4 K from the 2-K cold box to the 4.5-K liquefier system. In the latter case the Carnot efficiency of the 4.5-K liquefier system is increased by 1% to account for the refrigeration benefit given by the 2-K cold box stream. This will be discussed later. So

then, the equivalent input power required for the 4.5-K liquefier system is found by using the interfaces described, determining the reversible power required and dividing by the 4.5-K liquefier system Carnot efficiency.

The COP_{INV} is the ratio of total input power (as discussed above) to the heat into the helium II bath (i.e., the 'load' or 'heat load'). It is a more practically apparent measure of performance than the Carnot efficiency. Of course, the relationship between the COP_{INV} and Carnot efficiency is the ratio of the availability to the load to heat into the bath. Two different COP_{INV}'s are used in this study. The 'real' (or 'total process') COP_{INV} is based upon the total input power to the whole process. That is, the total input power to the 4.5-K liquefier system, LN pre-cooling (if applicable) and the 2-K vacuum pumping and compressor system. The 'ideal' (or 'cold box') COP_{INV} is based upon the availability to (i.e., the supply exergy flux minus the return exergy from) the 2-K cold box. It does not include the power inputs used for the real COP_{INV}, except that the availability provided by the LN pre-cooling (if applicable) is added to the availability provided to the 2-K cold box. These two COP_{INV}'s are helpful in examining the overall process exergy loss effects between the passive components (i.e., heat-exchangers and throttling-valves) and the active components (i.e., vacuum pumping system, compressor system and 4.5-K liquefier system).

The three varied process parameters are considered the key independent variables with which to study the COP_{INV}. As such the real COP_{INV} and ideal COP_{INV} are compared with respect to the flow ratio for each supply pressure and total heat exchanger NTU's. From this data, the conditions yielding the minimum real and ideal COP_{INV}'s can be studied.

2.7 Traditional Sub-Atmospheric Helium Processes

Small 2-K helium systems requiring less than 50 W (at around 2 K) for short duration testing, typically utilize direct (warm) vacuum pumping (with no refrigeration-recovery) to produce the cold sub-atmospheric helium. FIGURE 2.7.1 depicts such a process (labeled configuration C1). The 4.5-K helium liquefier system (labeled 4.5-K Plant) could also be a liquid helium dewar. However, as previously discussed, for the purposes of quantifying the equivalent input power a 4.5-K helium liquefier system is assumed to provide the 3 atm, 4.5 K helium make-up. The liquid boil-off due to the 2-K heat load (which is not shown going) into the helium II bath (labeled LOAD) and the flash from the throttling valve (which is referred to as a Joule-Thompson, or JT valve, and labeled JT) is warmed (without recovering any of the sub-atmospheric stream's refrigeration) close to ambient temperature (shown by an ambient vaporizer, labeled VAP). It is then compressed to slightly positive atmospheric pressure (say, 1.05 atm) by the vacuum pumping system (labeled VPS). From the vacuum pumping system the helium may be stored in gas bags (to be re-processed later) or sent back to the (compressor suction of the) 4.5-K plant.

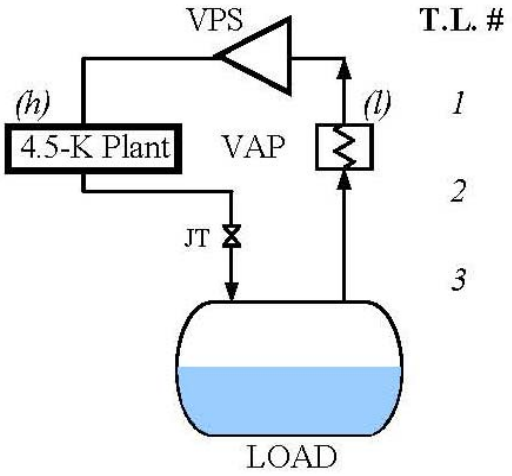

FIGURE 2.7.1 – Configuration C1

The ideal and real COP_{INV}'s for a direct vacuum pumping process (as shown in FIGURE 2.7.1), using a 4.5-K liquefier system with a Carnot efficiency of 10% and a vacuum pumping system isothermal efficiency of 14.5% (plus a motor efficiency of 90%), are about 700 W/W and 6500 W/W, respectively. Introducing a small heat exchanger, as depicted in FIGURE 2.7.2 [28] (i.e., configuration C1-A), can significantly improve the process COP_{INV}. This heat exchanger (labeled HX-1) is intended to recover a portion of the highly valuable sub-atmospheric stream refrigeration between 2.0 K and 4.5 K. The ideal and real COP_{INV}'s will decrease by 30% (to about 480 W/W and 4500 W/W, respectively) using a heat exchanger (HX-1) with 2 NTU's, but only (decrease) 35% (to about 450 W/W and 4200 W/W, respectively) for a heat exchanger with 6 NTU's. This process improvement is presented in FIGURE 2.7.3 as a plot of ideal and real COP_{INV}'s with respect to HX-1 NTU's. This heat exchanger's net effect is to reduce the enthalpy supplied to the load. So, a small heat exchanger of at least 2 NTU's is needed, and will improve the process performance considerably with a small pressure drop. Note that since the reversible input power required for the 4.5-K liquefier system and vacuum pumping system is (essentially) constant, the real and ideal COP_{INV}'s differ by a constant factor. The process configurations studied assume this particular heat exchanger (though it may have a different label) to have 5 NTU's. This assures that the optimal process performance condition is not hindered by this coldest heat exchanger.

These results provide an upper limit (worst case) on the COP_{INV} values to expect from the process configurations to be studied and allude to the dramatic effect that possible process configurations using simple passive components (heat exchangers, JT valves, etc.) may have on the process performance. As a lower limit (best case) on the

COP_{INV}, the performance of large efficient 2-K systems employing cold compressors is noted to be about 900 W/W (for the real COP_{INV}) [3].

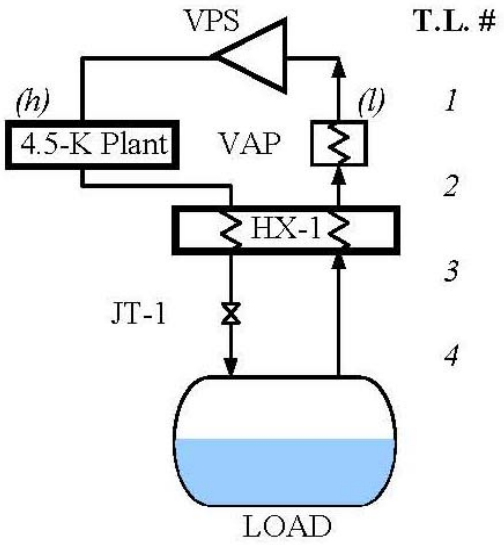

FIGURE 2.7.2 – Configuration C1-A

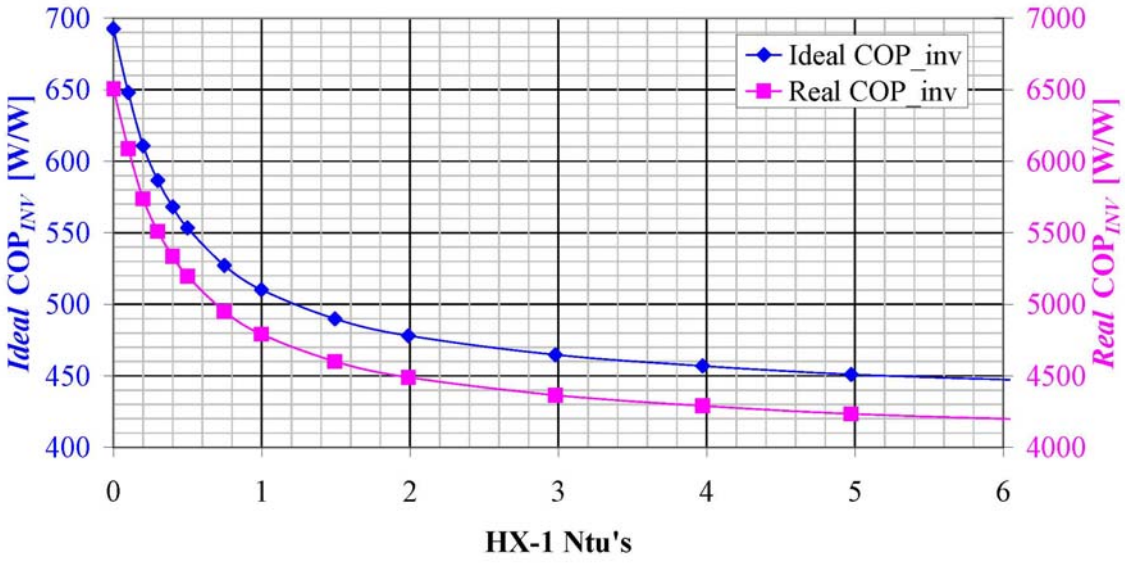

FIGURE 2.7.3 – Configuration C1-A HX-1 NTU's vs. COP_{INV}

2.8 Comparable 2-K Systems

As mentioned previously, the CTF at JLab and TTF at DESY are the only two 2-K systems found by the author that are comparable the objective of this study. Of these, only performance data on JLab's CTF is available (to the author). TABLE 2.8.1 summarizes the estimated performance parameters. However, it should be mentioned that due to a (mis-)implementation of the piping system, the actual performance is considerably less than indicated. As shown in TABLE 2.8.1, the performance of the 2-K system (if implemented properly) has a COP_{INV} of about 3400 W/W and a Carnot efficiency of about 5%.

TABLE 2.8.1 – JLab CTF Estimated 2-K Performance

2-K Load		
Temperature	2.09	[K]
Pressure	0.040	[atm]
Heat Load	140	[W]
Mass flow	9.0	[g/s]
Effective latent heat	15.5	[J/g]
Exergy	**24.5**	[kW]
4.5-K Liquefier System		
Compressors		
Input power	270	[kW]
LN System		
Mass flow	6.8	[g/s]
Carnot efficiency	35.0%	[-]
Equivalent input power	13.4	[kW]
Sub-Total	**284**	[kW]
Vacuum Pumping System		
Pressure ratio	42.8	[-]
Isothermal efficiency	14.2%	[-]
Input power	**149**	[kW]
2-K Compressor System		
Pressure ratio	13.8	[-]
Isothermal efficiency	38.0%	[-]
Input power	**38.9**	[kW]
Overall 2-K System		
Total input power	**471**	[kW]
COP_{INV}	3368	[W/W]
Carnot efficiency	5.2%	[-]

3. PROCESS MODEL SIMULATION

3.1 Model Simulation, Format and Parameters

Microsoft Excel and Visual Basic were chosen as the software to perform the process calculations. The fluid property routines are designed to be accessed as function calls from the worksheets. The Visual Basic routines written (see APPENDIX D for code outlines), which are available from the author, include the heat exchanger integrated cooling curve (for variable specific heat) analysis for calculating the:

(i) UA and NTU's given inlet process conditions, pressure drops, heat in-leak and either warm-end or cold-end stream temperature difference.

(ii) Outlet temperatures given inlet process conditions, pressure drops, heat in-leak and either UA, NTU's or effectiveness.

(iii) Maximum possible duty given the inlet process conditions, pressure drops and heat in-leak.

(iv) Common inlet or outlet temperature for a multi-stream heat exchanger (since these streams, although at the same temperature, may be at differing pressures).

The structure of each process calculation sheet is set-up in a grid format, and called a process stream matrix. That is, each process state point is designated by two indices. The first is the stream name; e.g., '*h*' for the high pressure stream to be cooled, 'ℓ' for the sub-atmospheric stream from the 2-K load, '*N*' for nitrogen (where LN pre-cooling is used), etc. The second index is the 'temperature level' (T.L.) number, where an increasing temperature level number indicates a decreasing temperature. So, in

general for the process stream matrix, moving from top to bottom represents a decreasing temperature, and moving from right to left represents an increasing pressure. Each calculation sheet also has areas for the pertinent parameters and inputs for each component (load, heat exchanger, vacuum pumping system, compressor, etc.), the exergy usage, and model energy and exergy balance checks.

The following are the parameters common to all model configurations to be discussed (some of which have not been mentioned previously); refer to APPENDIX E for a complete list of parameters.

(1) High pressure stream total pressure drop equal to 0.35 atm. The distribution of this pressure drop is proportional to the heat exchanger NTU's.

(2) 2-K system compressor suction pressure (and vacuum pumping system discharge pressure) equal to 1.05 atm.

(3) 2-K system compressor suction and discharge temperature as well as vacuum pumping system discharge temperature equal to 300 K.

(4) 2-K system compressor and vacuum pumping system motor efficiencies equal to 90%.

(5) 5 NTU's are used for the coldest heat exchanger, except for configuration C2-B.

(6) LN pre-cooling system Carnot efficiency equal to 35%.

Even though the primary focus of study is a 2-K helium refrigerator requiring a few grams per second of 4.5-K liquefaction make-up flow, in order to be consistent for comparison of the parameters in the study, all the analyses presented assume a total

return flow of 12 g/s at 0.0310 atm (i.e., 2.0 K). As such, there will be cases where the make-up flow is greater than 2 to 3 g/s. APPENDIX E is a complete list of the parameters and nomenclature used on the process sheets.

3.2 Model Methodology and Checks

Each model configuration has three types of energy balance checks that are verified to be within an acceptable fractional error of tolerance; typically $1x10^{-8}$. The first is that both the 'hot' and 'cold' heat exchanger stream duties are verified to be equal. Second, a control volume energy balance check is performed and verified to be zero. Third, an energy balance check between each temperature level and the load is performed. This involves balancing the enthalpy flux, heat input and work output from that temperature level to the highest (coldest) temperature level number. Also, an exergy check is performed between each temperature level and the load, involving balancing the exergy flux, and exergy losses (irreversibilities) from that temperature level to the highest (coldest) temperature level.

3.3 Model Configuration C2-A

Configuration C2-A [28] (FIGURE 3.3) consists of two heat exchangers, labeled HX-1 and HX-2. The refrigeration of the sub-atmospheric helium flow, returning from the 2-K load, is recovered using the heat exchangers to nearly ambient temperature, warmed to 300 K using the ambient vaporizer and then compressed to atmospheric pressure (also referred to as 'slightly positive pressure') by the vacuum pumping system. A portion of the atmospheric helium flow is diverted to the 4.5-K plant, with the

remaining flow compressed by the (2-K system) compressor (labeled RSC). Note that this compressor system is handling flow from the 2-K load and is not the same as the compressor system integrated into the 4.5-K helium liquefier system. The super-critical 4.5 K helium from the 4.5-K plant is injected between the two heat exchangers and downstream of JT-1.

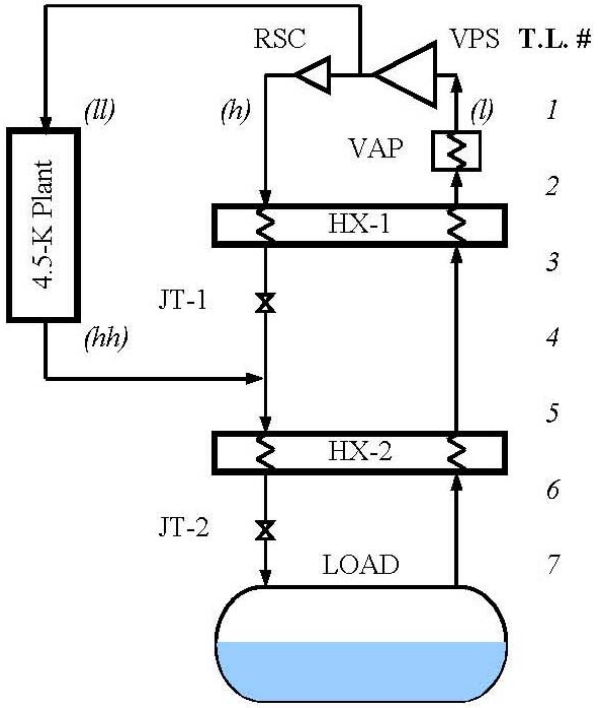

FIGURE 3.3 – Configuration C2-A

By diverting a portion of the flow compressed by the vacuum pumping system to the 4.5-K plant, a flow imbalance is created in HX-1. As mentioned previously, this flow imbalance (or flow ratio) is one of the key varied parameters. This flow imbalance serves to compensate for losses due to finite heat exchanger size, the higher heat capacity of the high pressure stream and the heat in-leaks. For every case, the length of HX-2 is fixed at 5 NTU's. In general, the temperature upstream of the 4.5-K plant injection may be considerably higher than 4.5 K. Also, note that the throttling across JT-1 will often result

in a warmer temperature since the process conditions will usually result in a negative Joule-Thompson coefficient.

3.4 Model Configuration C2-A-p

Configuration C2-A-p [28] (FIGURE 3.4) is similar to configuration C2-A except that it uses liquid nitrogen (LN) to pre-cool the high-pressure stream, then sends the 80-K (instead of 300-K) helium into the 4.5-K plant. HX-1 recovers a portion of the sub-atmospheric flow refrigeration and the saturated nitrogen vapor sensible heat. HX-2 is the LN boiler. So, ignoring HX-1 and HX-2 (and the liquid nitrogen), configuration C2-A-p would diagrammatically look just like C2-A. Note that the 80-K high pressure helium is throttled before going to the 4.5-K plant. This is a practical consequence of the difficulty in matching the pressures of the 2-K cold box and 4.5-K plant high-pressure streams (of which, the 4.5-K plant high pressure stream will usually be at a higher pressure). The Carnot efficiency of the 4.5-K plant was increased by 1% (from 10% used on other configurations without LN pre-cooling, to 11%) as a consequence of the cooling provided by the 80-K helium sent to the 4.5-K plant. Refer to APPENDIX F for the method used to estimate this increase.

Obviously, at some (lower) flow ratio, the use of LN is not necessary. The performance of this process configuration was not studied below this point. It is important to mention that all configurations require purification of the sub-atmospheric flow. This can be easily integrated into the C2-A-p process as compared to the others.

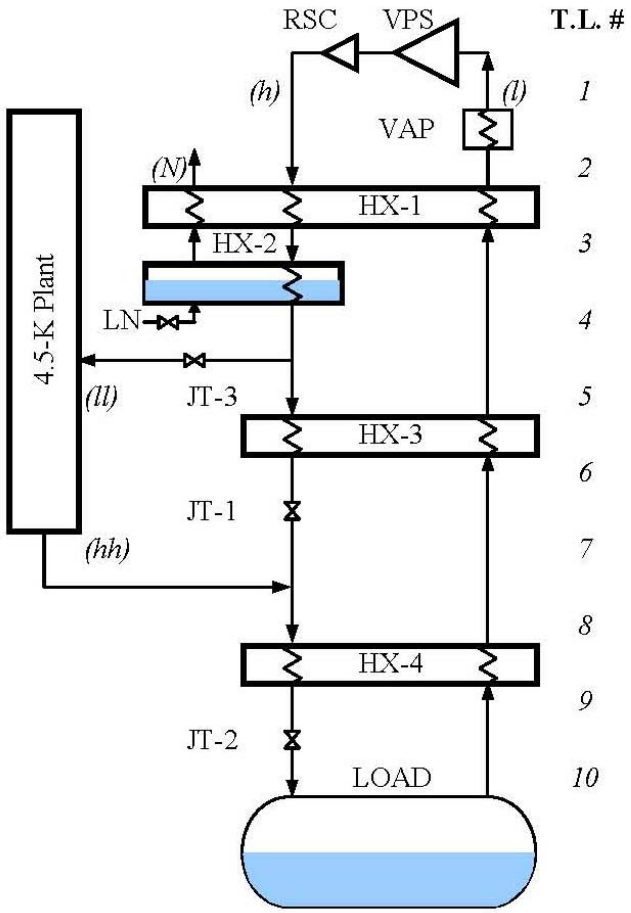

FIGURE 3.4 – Configuration C2-A-p

3.5 Model Configuration C2-B

Configuration C2-B [28], as shown in FIGURE 3.5, is similar to C2-A except that the coldest heat exchanger is sub-divided into HX-2A and HX-2B, where the high-pressure flow is recycled through HX-2A/B to take advantage of the real fluid specific heat difference between the high and sub-atmospheric pressure streams. Unlike HX-1, for a good portion of HX-2A/B, the specific heat of the high pressure stream is less than the sub-atmospheric stream. Note that the cold injection from JT-1 and the 4.5-K plant injection are switched, depending upon whether the high pressure stream (‘*h*’) enthalpy out of HX-2B is less than or more than the enthalpy from the 4.5-K plant (which is

fixed). The length of HX-2A/B is not fixed at 5 NTU's, since this would over-constrain the problem. Rather, the NTU's of HX-2A plus HX-2B are prohibited from exceeding 5 NTU's, while the total heat exchanger NTU's (for HX-1, HX-2A and HX-2B) are required to be as specified (i.e., recall that the total heat exchanger NTU's is a varied process parameter).

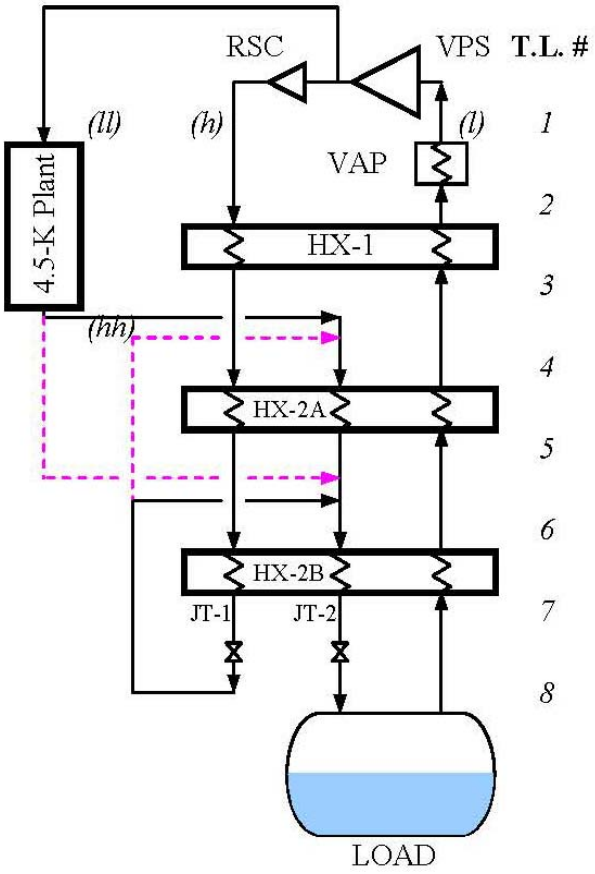

FIGURE 3.5 – Configuration C2-B

4. PROCESS MODEL RESULTS

4.1 Optimal Performance

FIGURES 4.1.1 to 4.1.6 [28] present the results of the ideal and real COP_{INV}'s, for the three configurations shown in FIGURES 3.3, 3.4 and 3.5. The COP_{INV}'s in these figures are for the varying flow ratios (labeled $\xi_{h\ell}$) at a supply pressure of 12 atm, and for 20, 25, 30, 35, 40 and 45 total heat exchanger NTU's. Though not presented, calculations were also made for supply pressures of 6, 9, 15 and 18 atm, in order to determine values yielding optimal performance. The results at other supply pressures are quite similar in their nature and trend to those presented, in that the COP_{INV} increases very quickly for flow ratios greater than the optimum flow ratio (which yields the minimum COP_{INV}), but increases only gradually for flow ratios less than the optimum. For configurations C2-A and C2-A-p, the 'knees' of the (constant NTU) curves are sharper than are those for configuration C2-B.

FIGURES 4.1.7 to 4.1.9 [28] and TABLES 4.1.7 to 4.1.12 present the optimum (minimum) ideal COP_{INV}'s and their associated flow ratio values vs. the total heat exchanger NTU's at various supply pressures (labeled $p_{h,1}$) for configurations C2-A, C2-B and C2-A-p, respectively. FIGURES 4.1.10 to 4.1.12 [28] and TABLES 4.1.13 to 4.1.18 present similar data but for the optimum (minimum) real COP_{INV}. Overall, the general and optimum performances of all three configurations are quite similar and relatively close. However, it should be noticed that the optimum real COP_{INV}'s for configuration C2-A-p are less than C2-A (and C2-B), but the optimum ideal COP_{INV}'s for C2-A-p are greater than C2-A (and C2-B).

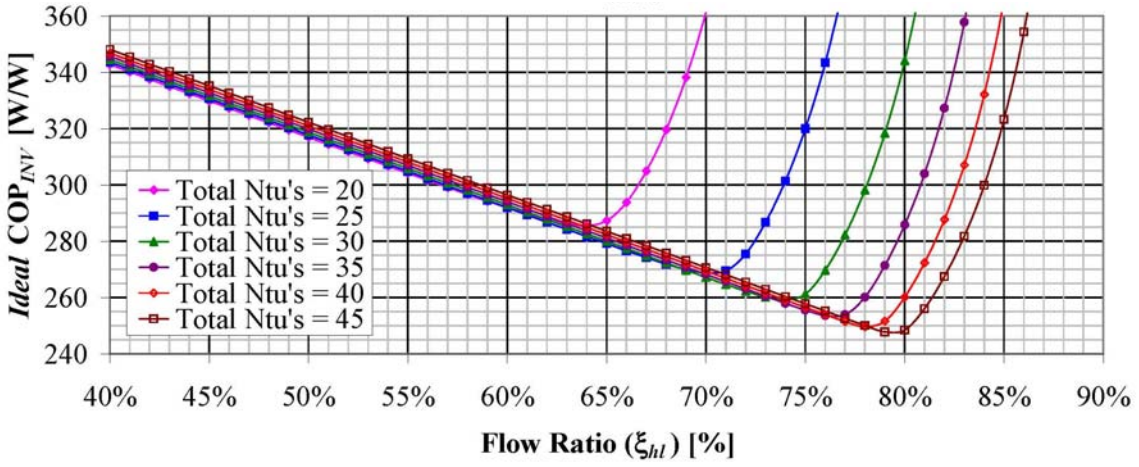

FIGURE 4.1.1 – C2-A Ideal COP_{INV} vs. Flow Ratio (ξ_{hl})

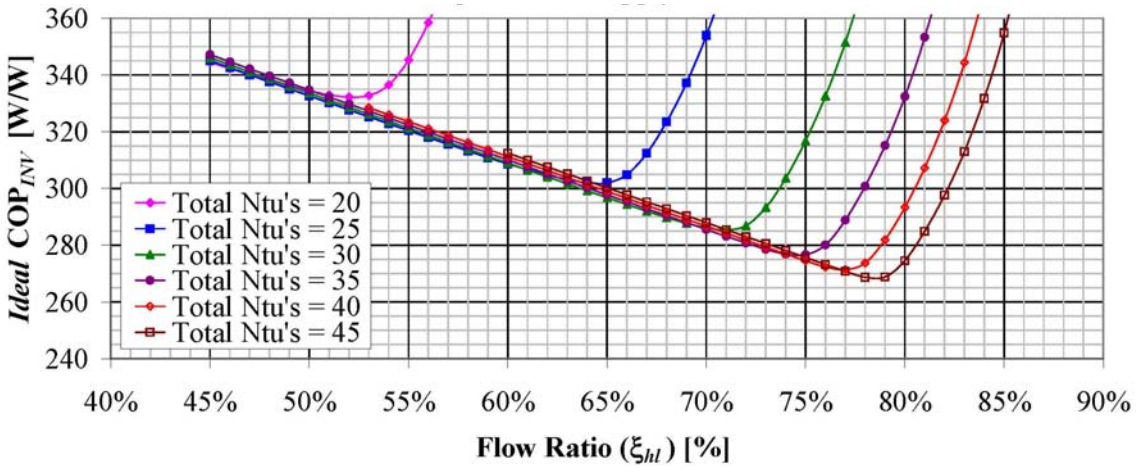

FIGURE 4.1.2 – C2-A-p Ideal COP_{INV} vs. Flow Ratio (ξ_{hl})

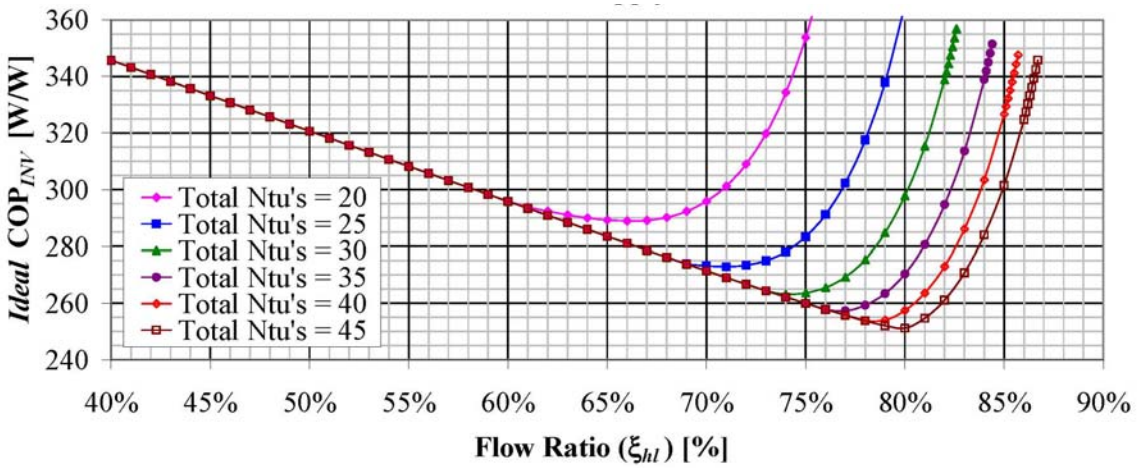

FIGURE 4.1.3 – C2-B Ideal COP_{INV} vs. Flow Ratio (ξ_{hl})

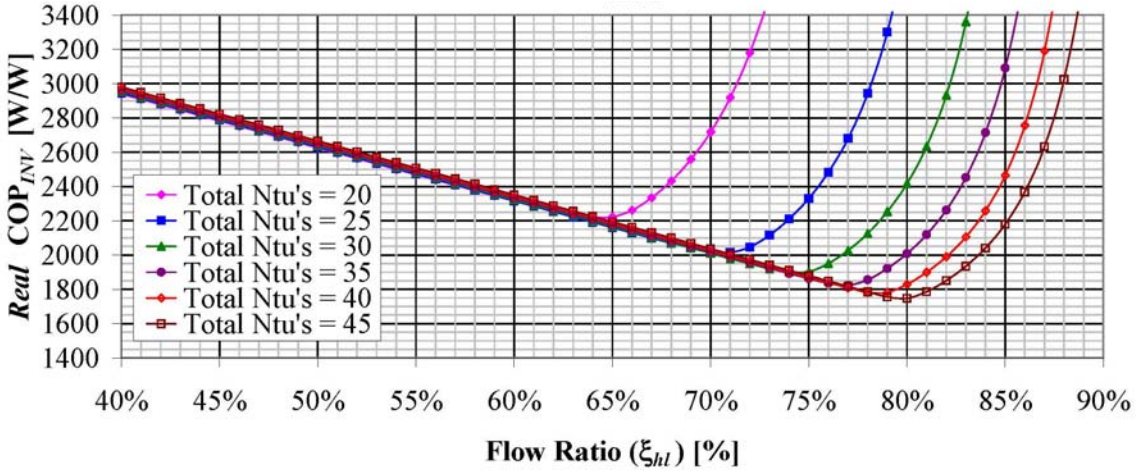

FIGURE 4.1.4 – C2-A Real COP_{INV} vs. Flow Ratio (ξ_{hl})

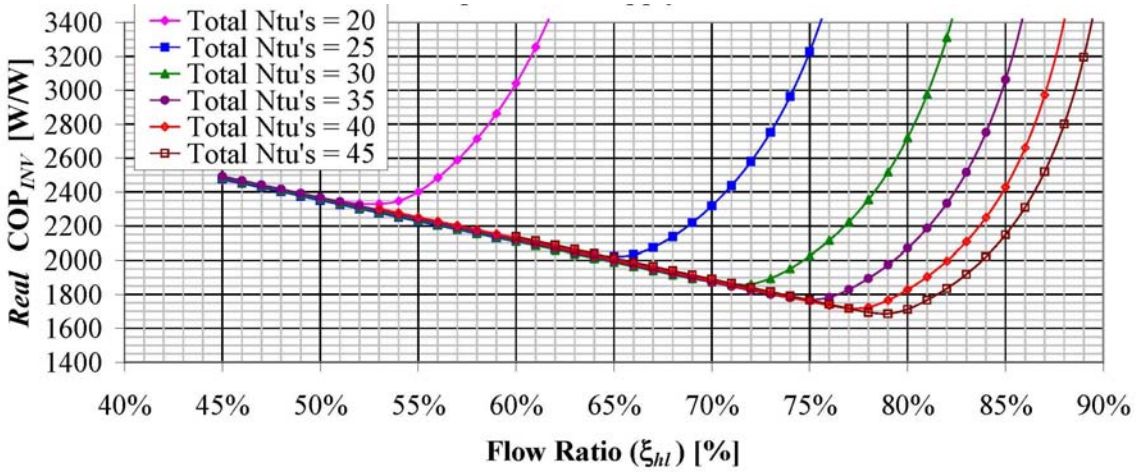

FIGURE 4.1.5 – C2-A-p Real COP_{INV} vs. Flow Ratio (ξ_{hl})

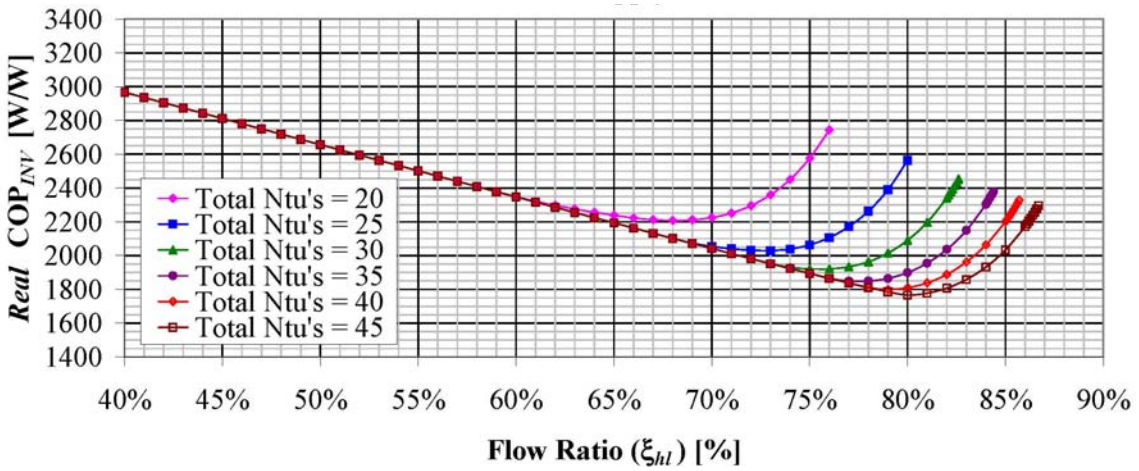

FIGURE 4.1.6 – C2-B Real COP_{INV} vs. Flow Ratio (ξ_{hl})

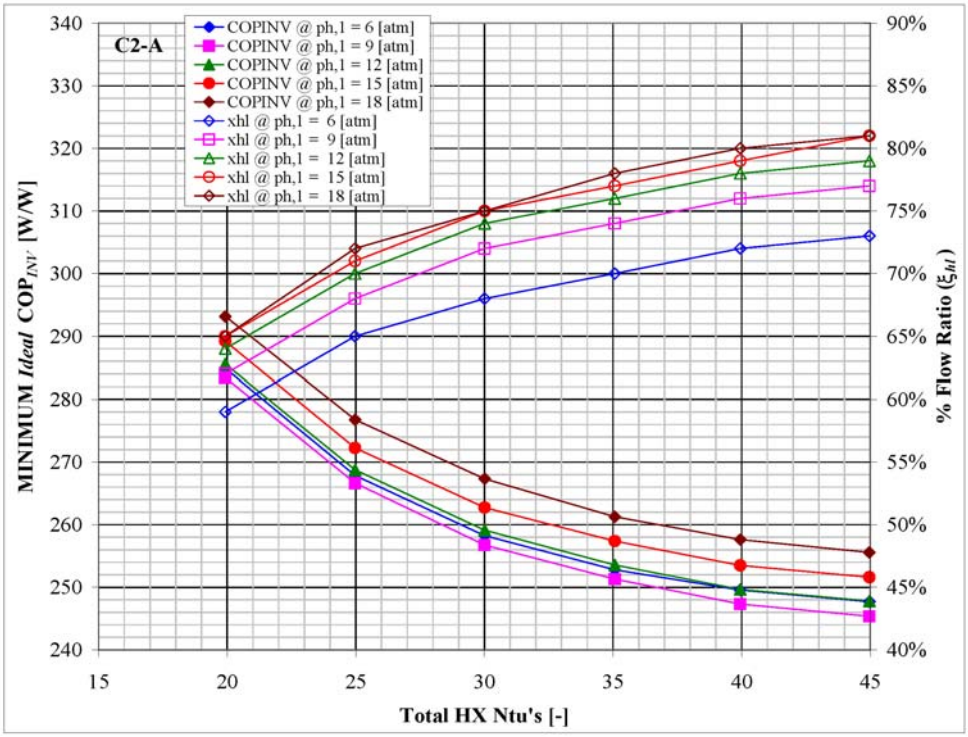

FIGURE 4.1.7 – C2-A Minimum Ideal COP_{INV} vs. Total NTU's

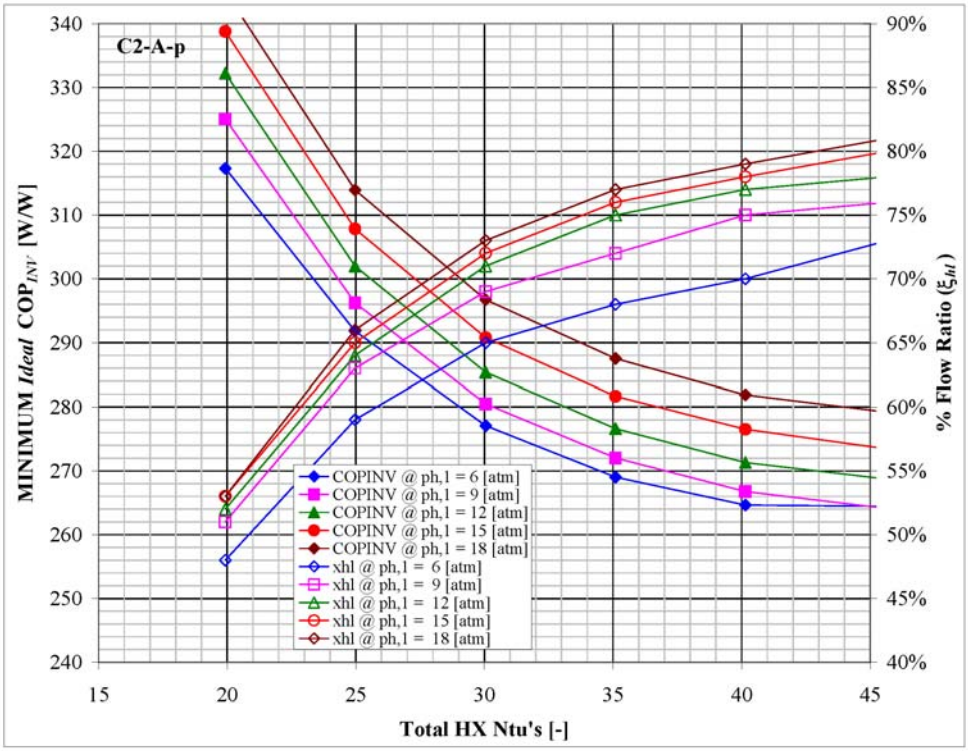

FIGURE 4.1.8 – C2-A-p Minimum Ideal COP_{INV} vs. Total NTU's

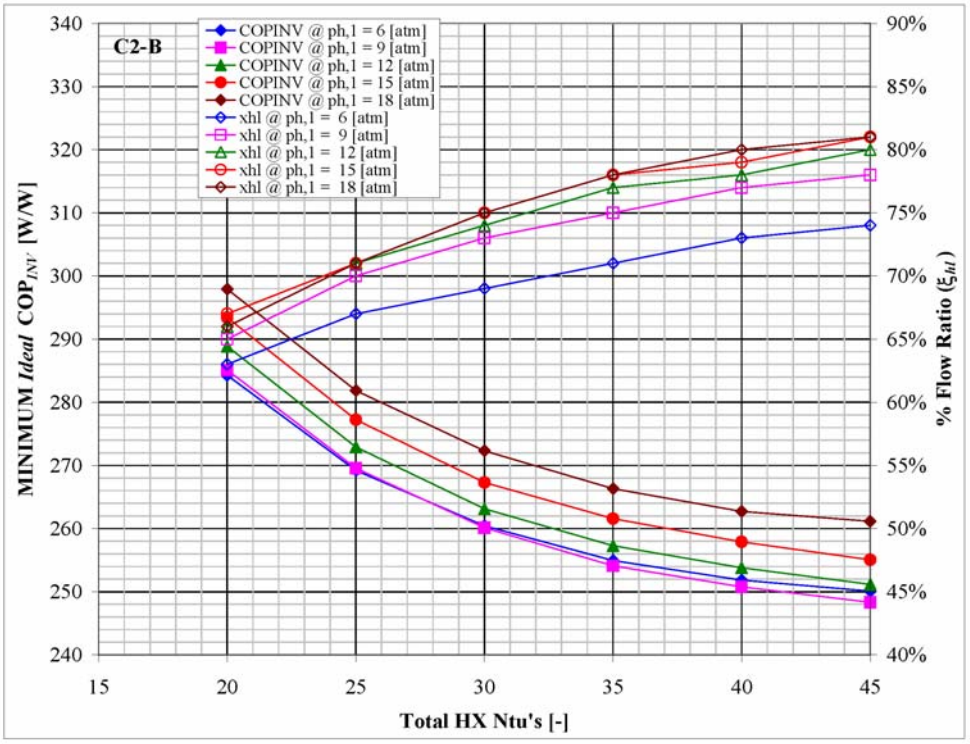

FIGURE 4.1.9 – C2-B Minimum Ideal COP_{INV} vs. Total NTU's

TABLE 4.1.7 – C2-A Minimum Ideal COP_{INV} vs. Total NTU's

C2-A	**COP_{INV} @ $p_{h,1}$ =**				
Total Ntu's	**6 [atm]**	**9 [atm]**	**12 [atm]**	**15 [atm]**	**18 [atm]**
20	284.9	283.4	285.6	289.2	293.2
25	267.8	266.6	268.8	272.2	276.8
30	258.2	256.7	259.1	262.7	267.3
35	252.8	251.3	253.6	257.4	261.2
40	249.5	247.3	249.6	253.5	257.6
45	247.7	245.3	247.8	251.6	255.5

This is explained by recalling that the 4.5-K plant Carnot efficiency is higher for configuration C2-A-p, resulting in a lower real COP_{INV} (as compared to configurations C2-A and C2-B). Likewise, the exergy loss due to throttling the high pressure 80K stream from the 2-K cold box into the 4.5-K plant results in a higher ideal COP_{INV} for configuration C2-B (as compared to configurations C2-A and C2-A-p).

TABLE 4.1.8 – C2-A Flow Ratio (ξ_{hl}) at Minimum Ideal COP_{INV}

C2-A	ξ_{hl} @ $p_{h,1}$ =				
Total Ntu's	**6 [atm]**	**9 [atm]**	**12 [atm]**	**15 [atm]**	**18 [atm]**
20	59%	62%	64%	65%	65%
25	65%	68%	70%	71%	72%
30	68%	72%	74%	75%	75%
35	70%	74%	76%	77%	78%
40	72%	76%	78%	79%	80%
45	73%	77%	79%	81%	81%

TABLE 4.1.9 – C2-A-p Minimum Ideal COP_{INV} vs. Total NTU's

C2-A-p	COP_{INV} @ $p_{h,1}$ =				
Total Ntu's	**6 [atm]**	**9 [atm]**	**12 [atm]**	**15 [atm]**	**18 [atm]**
20	317.3	325.1	332.2	338.8	345.0
25	291.8	296.2	302.0	307.8	313.9
30	277.1	280.5	285.4	290.8	296.7
35	269.0	272.0	276.6	281.7	287.5
40	264.6	266.7	271.3	276.5	281.9
45	264.4	264.1	268.7	273.4	279.2

TABLE 4.1.10 – C2-A-p Flow Ratio (ξ_{hl}) at Minimum Ideal COP_{INV}

C2-A-p	ξ_{hl} @ $p_{h,1}$ =				
Total Ntu's	**6 [atm]**	**9 [atm]**	**12 [atm]**	**15 [atm]**	**18 [atm]**
20	48%	51%	52%	53%	53%
25	59%	63%	64%	65%	66%
30	65%	69%	71%	72%	73%
35	68%	72%	75%	76%	77%
40	70%	75%	77%	78%	79%
45	73%	76%	78%	80%	81%

TABLE 4.1.11 – C2-B Minimum Ideal COP_{INV} vs. Total NTU's

C2-B	**COP_{INV} @ $p_{h,1}$ =**				
Total Ntu's	**6 [atm]**	**9 [atm]**	**12 [atm]**	**15 [atm]**	**18 [atm]**
20	284.3	285.1	288.8	293.4	297.9
25	269.2	269.5	272.9	277.2	281.8
30	260.4	260.1	263.1	267.3	272.3
35	254.9	254.1	257.3	261.6	266.3
40	251.8	250.8	253.8	257.9	262.7
45	250.1	248.3	251.2	255.0	261.1

TABLE 4.1.12 – C2-B Flow Ratio (ξ_{hl}) at Minimum Ideal COP_{INV}

C2-B	**ξ_{hl} @ $p_{h,1}$ =**				
Total Ntu's	**6 [atm]**	**9 [atm]**	**12 [atm]**	**15 [atm]**	**18 [atm]**
20	63%	65%	66%	67%	66%
25	67%	70%	71%	71%	71%
30	69%	73%	74%	75%	75%
35	71%	75%	77%	78%	78%
40	73%	77%	78%	79%	80%
45	74%	78%	80%	81%	81%

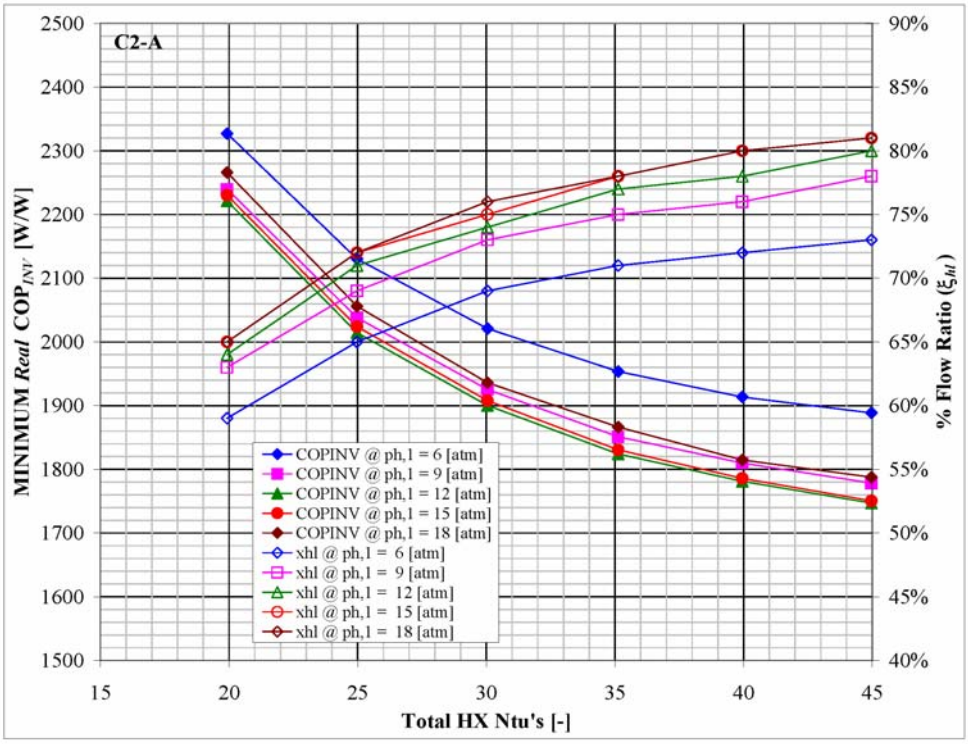

FIGURE 4.1.10 – C2-A Minimum Real COP$_{INV}$ vs. Total NTU's

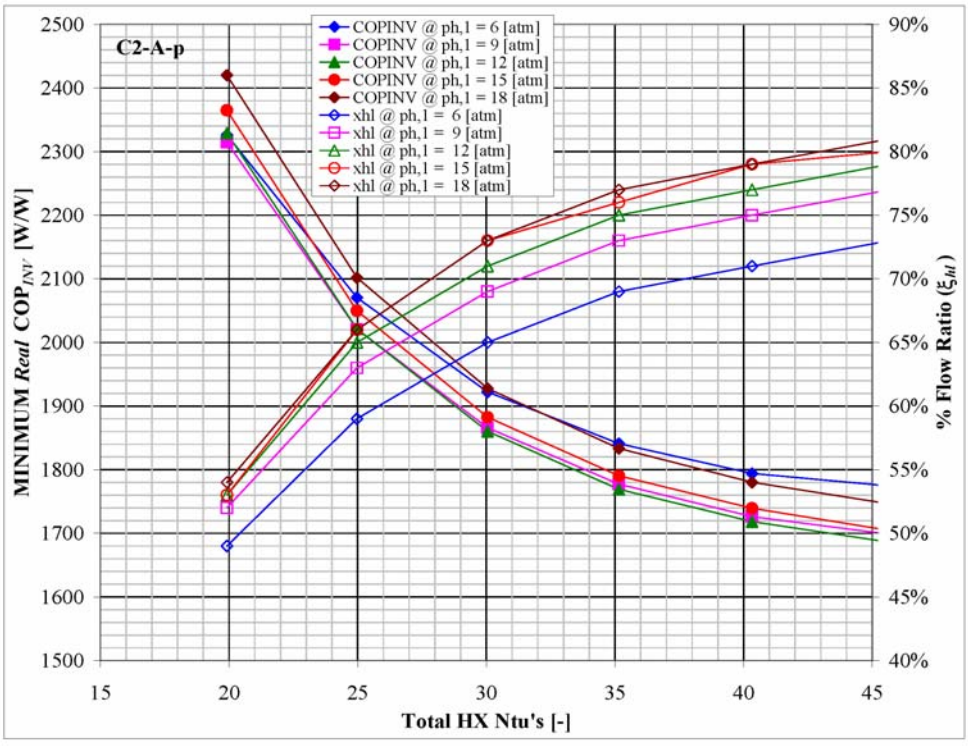

FIGURE 4.1.11 – C2-A-p Minimum Real COP$_{INV}$ vs. Total NTU's

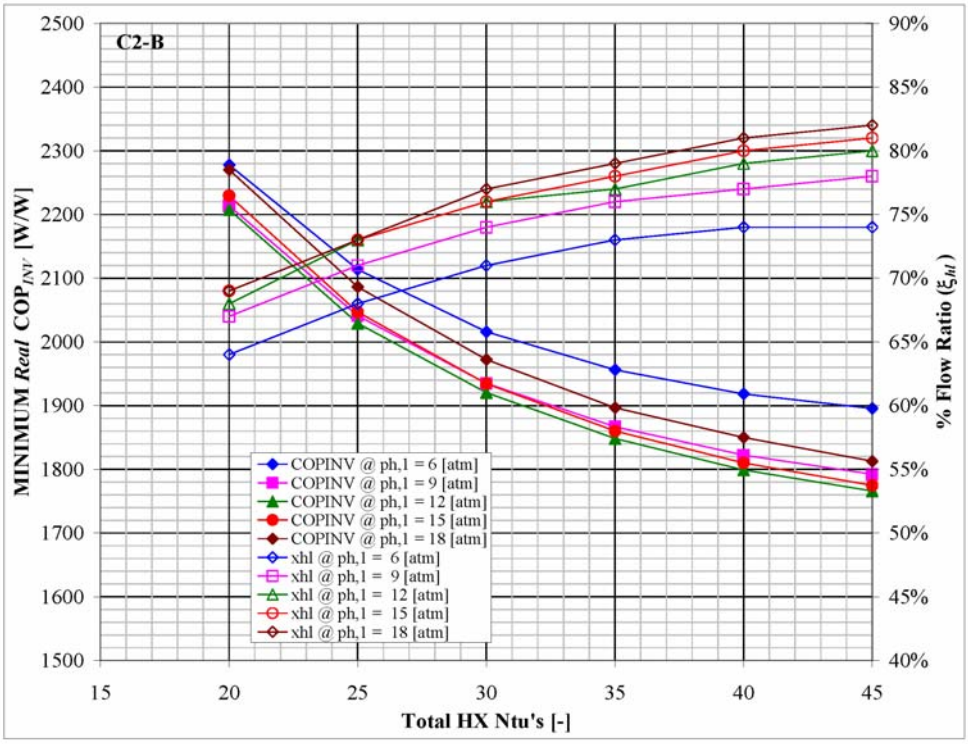

FIGURE 4.1.12 – C2-B Minimum Real COP_{INV} vs. Total NTU's

TABLE 4.1.13 – C2-A Minimum Real COP_{INV} vs. Total NTU's

C2-A	**COP_{INV} @ $p_{h,1}$ =**				
Total Ntu's	**6 [atm]**	**9 [atm]**	**12 [atm]**	**15 [atm]**	**18 [atm]**
20	2327	2240	2221	2230	2266
25	2130	2038	2014	2024	2056
30	2021	1925	1900	1908	1936
35	1953	1851	1824	1830	1866
40	1913	1810	1781	1786	1815
45	1888	1778	1747	1751	1787

TABLE 4.1.14 – C2-A Flow Ratio (ξ_{hl}) at Minimum Real COP_{INV}

C2-A	ξ_{hl} @ $p_{h,1}$ =				
Total Ntu's	**6 [atm]**	**9 [atm]**	**12 [atm]**	**15 [atm]**	**18 [atm]**
20	59%	63%	64%	65%	65%
25	65%	69%	71%	72%	72%
30	69%	73%	74%	75%	76%
35	71%	75%	77%	78%	78%
40	72%	76%	78%	80%	80%
45	73%	78%	80%	81%	81%

TABLE 4.1.15 – C2-A-p Minimum Real COP_{INV} vs. Total NTU's

C2-A-p	COP_{INV} @ $p_{h,1}$ =				
Total Ntu's	**6 [atm]**	**9 [atm]**	**12 [atm]**	**15 [atm]**	**18 [atm]**
20	2326	2314	2329	2365	2420
25	2070	2021	2021	2050	2102
30	1922	1866	1860	1882	1928
35	1841	1777	1769	1790	1833
40	1794	1726	1718	1739	1780
45	1774	1698	1686	1704	1746

TABLE 4.1.16 – C2-A-p Flow Ratio (ξ_{hl}) at Minimum Real COP_{INV}

C2-A-p	ξ_{hl} @ $p_{h,1}$ =				
Total Ntu's	**6 [atm]**	**9 [atm]**	**12 [atm]**	**15 [atm]**	**18 [atm]**
20	49%	52%	53%	53%	54%
25	59%	63%	65%	66%	66%
30	65%	69%	71%	73%	73%
35	69%	73%	75%	76%	77%
40	71%	75%	77%	79%	79%
45	73%	77%	79%	80%	81%

TABLE 4.1.17 – C2-B Minimum Real COP_{INV} vs. Total NTU's

C2-B	**COP_{INV} @ $p_{h,1}$ =**				
Total Ntu's	**6 [atm]**	**9 [atm]**	**12 [atm]**	**15 [atm]**	**18 [atm]**
20	2278	2214	2208	2229	2270
25	2114	2041	2029	2047	2086
30	2016	1935	1920	1934	1972
35	1956	1867	1848	1860	1896
40	1918	1822	1799	1810	1850
45	1895	1792	1766	1775	1813

TABLE 4.1.18 – C2-B Flow Ratio (ξ_{hl}) at Minimum Real COP_{INV}

C2-B	**ξ_{hl} @ $p_{h,1}$ =**				
Total Ntu's	**6 [atm]**	**9 [atm]**	**12 [atm]**	**15 [atm]**	**18 [atm]**
20	64%	67%	68%	69%	69%
25	68%	71%	73%	73%	73%
30	71%	74%	76%	76%	77%
35	73%	76%	77%	78%	79%
40	74%	77%	79%	80%	81%
45	74%	78%	80%	81%	82%

The difference between the optimum real COP_{INV}'s for configurations C2-A and C2-A-p indicates the sensitivity of the 4.5-K liquefier system Carnot efficiency (on the real process). For instance, at a supply pressure of 12 atm and for total heat exchanger NTU's of 40, the fractional difference between the real COP_{INV}'s of the two configurations is about 3.5% for a 10% fractional difference in 4.5-K liquefier system Carnot efficiency.

So, for (reasonable) heat exchanger sizes above 30 total NTU's and supply pressures greater than 9 atm, the optimum flow ratio is roughly 70 to 80% with a corresponding ideal COP_{INV} of 250 to 300 W/W and real COP_{INV} of 1750 to 1950 W/W. The process performance at the optimum flow ratio and 45 NTU's was a real COP_{INV} of

roughly 1750 W/W for configurations C2-A and C2-B and a real COP_{INV} of roughly 1690 W/W for configuration C2-A-p. The optimum process performance (i.e., minimum COP_{INV}) is primarily governed by the total number of heat exchanger NTU's and secondly by the supply pressure. An increase in total heat exchanger NTU's always increases the process performance.

For the ideal process at the optimum flow ratio, a supply pressure of either 9 or 6 atm always yielded better performance as compared to a supply pressure of 15 or 18 atm. For the real process at the optimum flow ratio, a supply pressure of 12 atm always yielded better performance as compared to a supply pressure of 18 or 6 atm. The reason for the more favorable real process performance at a supply pressure of 12 atm, rather than the optimal and lower supply pressure of 9 or 6 atm for the ideal process, is that the real process optimal flow ratio was slightly higher. This can be explained by recalling that the 4.5-K plant holds a larger influence on the real process efficiency than the compressor. The 4.5-K plant input power is directly related to one minus the flow ratio; and the compressor input power is directly related to the supply pressure. Keeping in mind that the real and ideal process optimums are not far from each other, at these close proximities the higher flow ratio is more influential on the real process, and the lower supply pressure is more influential on the ideal process.

APPENDIX G presents the process sheet calculations for the real process optimum flow ratio with a total of heat exchanger size of 40 NTU's and at a supply pressure of 12 atm.

4.2 General Results

FIGURES 4.2.1 to 4.2.3 show the distribution of the availability (exergy) given to the 2-K cold box for configurations C2-A, C2-A-p and C2-B at the minimum real COP_{INV} with total heat exchanger NTU's of 40 and at a supply pressure of 12 atm. These show that the exergy (usefully) used by the 2-K load is roughly 60% of the total availability to the 2-K cold box for configurations C2-A and C2-B and roughly 55% of the total availability to the 2-K cold box for configuration C2-A-p. Unsurprisingly, the major loss component (for the 2-K cold box) is the warm(er) heat exchanger that is imbalanced (i.e., HX-1 in configurations C2-A and C2-B and HX-3 in configuration C2-A-p).

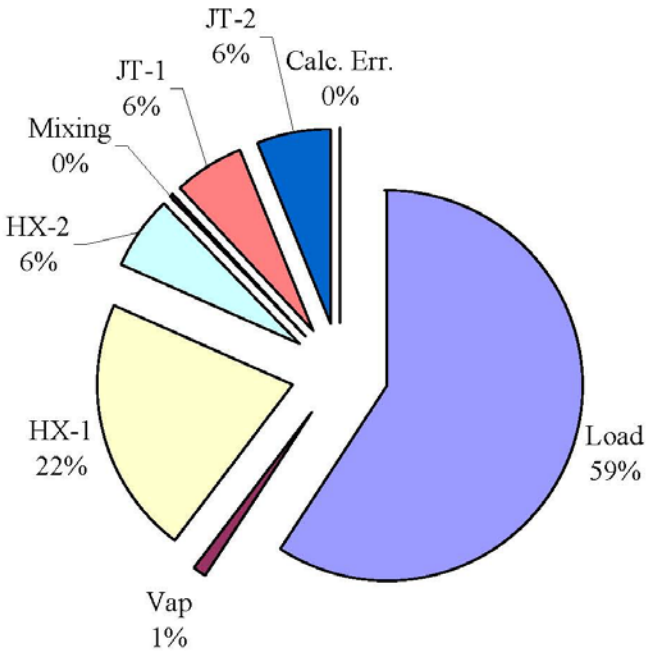

FIGURE 4.2.1 – C2-A Availability Given to the 2-K Cold Box

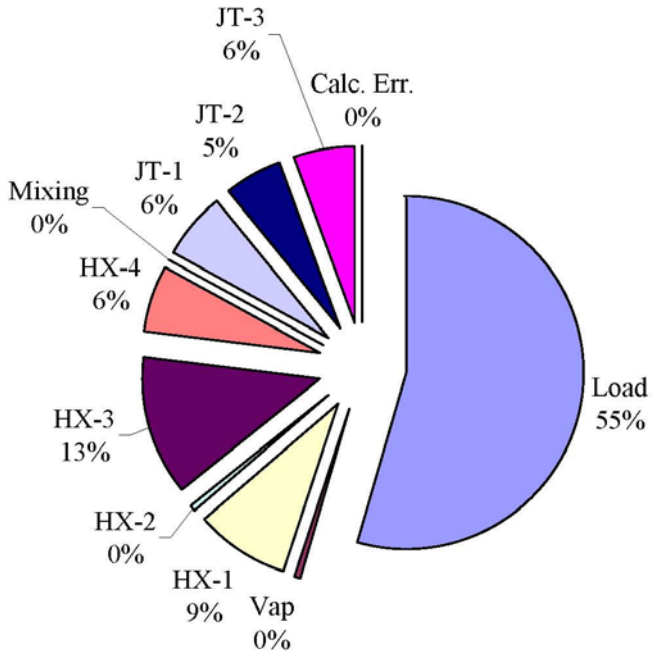

FIGURE 4.2.2 – C2-A-p Availability Given to the 2-K Cold Box

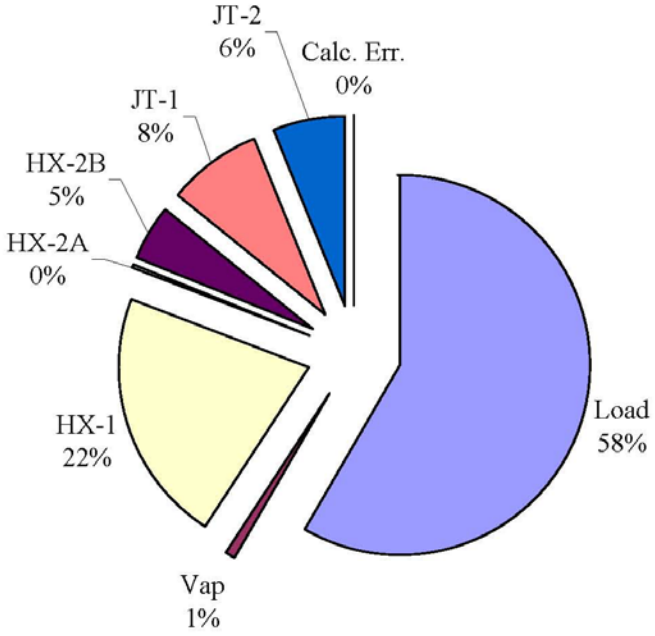

FIGURE 4.2.3 – C2-B Availability Given to the 2-K Cold Box

FIGURES 4.2.4 to 4.2.6 show the distribution of the real process input power usage (useful and non-useful) for configurations C2-A, C2-A-p and C2-B at the minimum real COP_{INV} with total heat exchanger NTU's of 40 and at a supply pressure of

12 atm. These show that the portion of input power actually (usefully) used by the 2-K load is roughly 8%. In the case of configuration C2-A, the components comprising the major loss (i.e., un-useful usage of input power) are the vacuum pumping system at roughly 44%, the 4.5-K plant at roughly 37%, the compressor system at roughly 5%, and then the 2-K cold box (labeled 2-K CBX) comprising the balance of roughly 6%. Losses for configuration C2-B are similar.

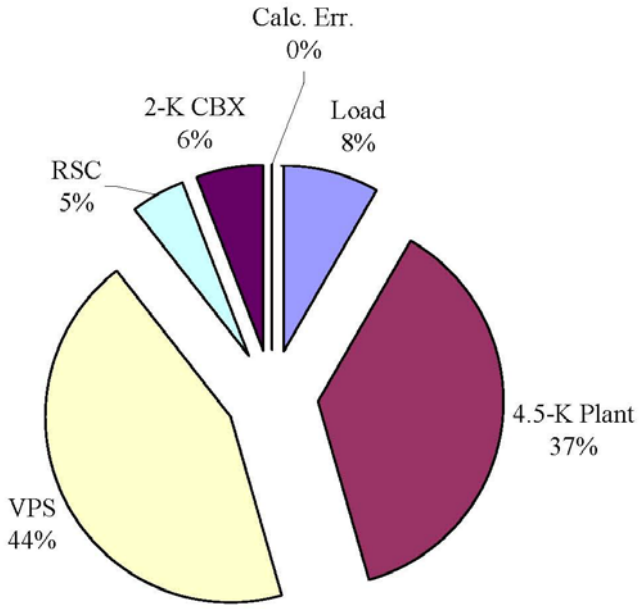

FIGURE 4.2.4 – C2-A Real Process Input Power Usage

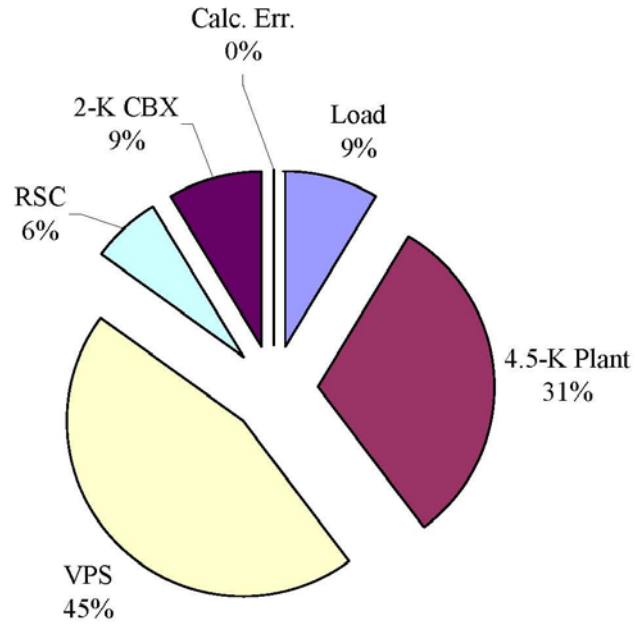

FIGURE 4.2.5 – C2-A-p Real Process Input Power Usage

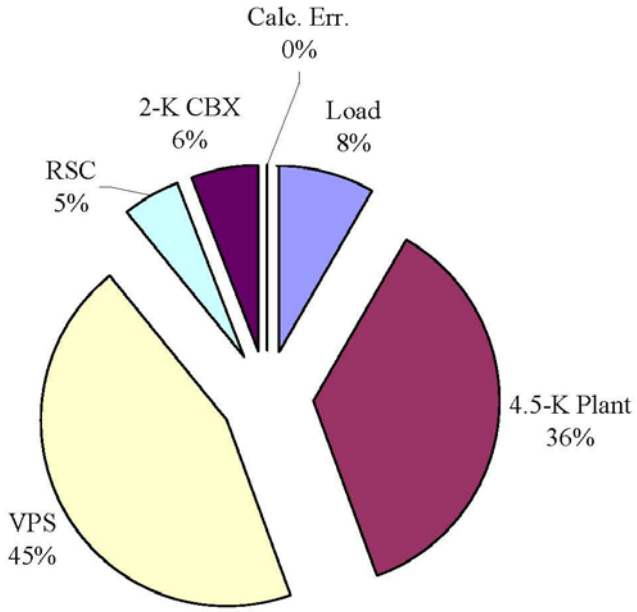

FIGURE 4.2.6 – C2-B Real Process Input Power Usage

The 2-K cold box loss is higher for configuration C2-A-p (roughly 9% as compared to about 6% for C2-A and C2-B) due to LN system and JT-3 losses. However, recall that the real COP_{INV} of configuration C2-A-p is higher than C2-A or C2-B due to

the higher 4.5-K plant Carnot efficiency (despite the flow ratio at the optimum performance being less).

FIGURES 4.2.7 and 4.2.8 present the cooling curves for configuration C2-A at the real process optimal flow ratio (78%) with total heat exchanger NTU's of 40 and at a supply pressure of 12 atm. As opposed to the typical constant fluid specific heat assumption (used in engineering heat exchanger analysis), these clearly show the non-constant behavior of the real fluid. TABLE 4.2 presents the distribution of exergy loss for these heat exchangers [27].

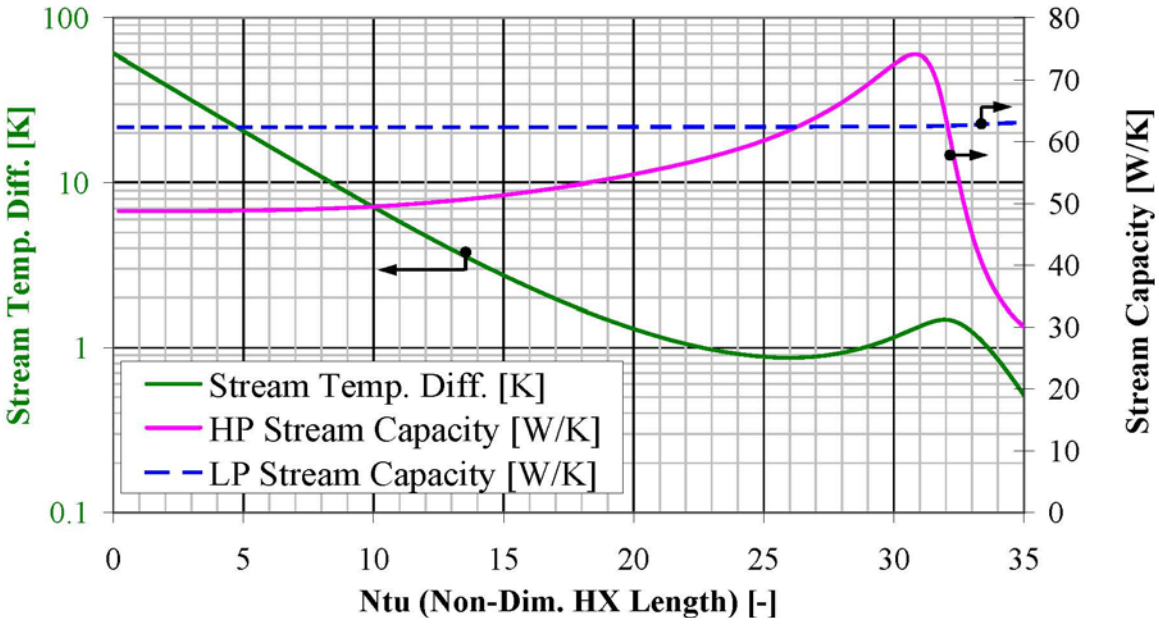

FIGURE 4.2.7 – C2-A HX-1 Cooling Curve

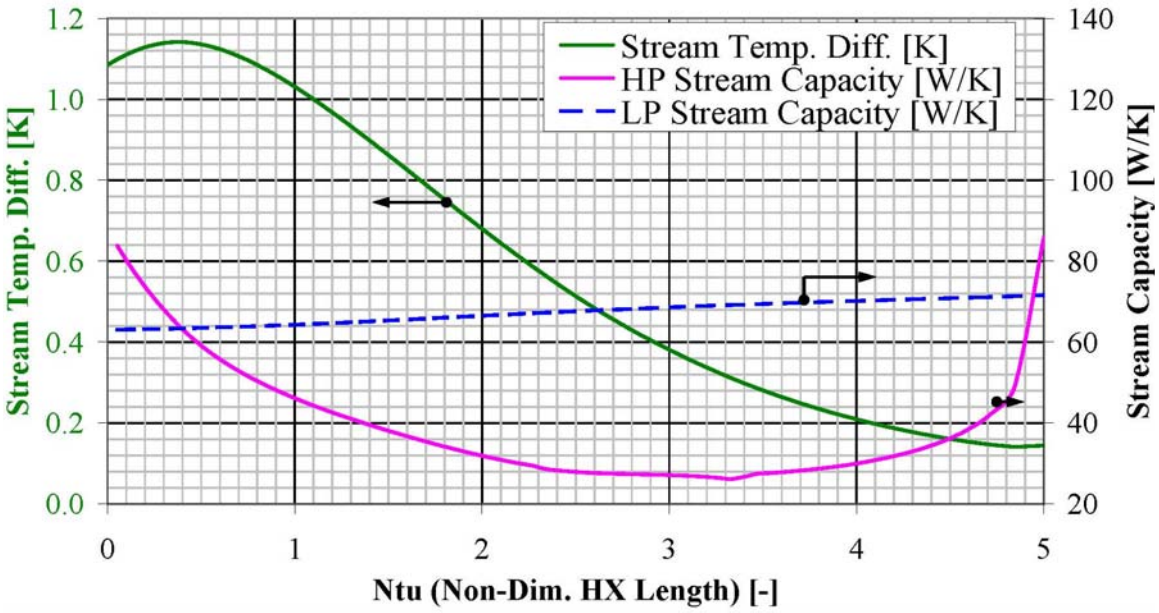

FIGURE 4.2.8 – C2-A HX-2 Cooling Curve

TABLE 4.2 – C2-A HX-1 and HX-2 Exergy Loss Distribution

		HX-1	HX-2
Total Exergy Loss	[kW]	13.08	3.71
Loss Due to Temperature Difference	[-]	50.8%	66.3%
Loss Due to Pressure Drop	[-]	14.4%	6.1%
Loss Due to Heat In-Leak	[-]	34.9%	27.2%

In FIGURE 4.2.7 (for HX-1) the range where the high pressure (labeled HP) stream capacity is greater than the sub-atmospheric (labeled LP) stream capacity is between (roughly) 13 to 7.5 K (for the HP stream), with the peak high pressure stream capacity at around 9 K. The high pressure stream capacity is less than the sub-atmospheric stream capacity for most of the heat exchanger length, but this is due to the flow imbalance. Also, as one would expect, the sub-atmospheric stream capacity is nearly constant (for a very low pressure gas). Notice that this cooling curve has two inflection points.

In FIGURE 4.2.8 (for HX-2) even though both high pressure and sub-atmospheric stream mass flow rates are equal, the high pressure stream capacity is less than the sub-atmospheric stream for most of the heat exchanger length; except at the ends. This accentuates the motivation for studying configuration C2-B. Also, notice that this cooling curve has two inflection points.

For configuration C2-B, it is worth noting that even though recycling the high-pressure flow through JT-1 (referring to FIGURE 3.5) back through HX-2 reduces the total heat exchanger exergy loss by increasing the high pressure stream capacity, the throttling through JT-1 (at a lower temperature) costs more exergy than was saved.

For configurations C2-A and C2-B, the sub-atmospheric stream temperature exiting the warmest heat exchanger (i.e., HX-1) is still quite cold (say roughly 240 K) and as such the ambient air vaporizer duty is roughly 25% of HX-1's duty (see FIGURES 3.3 to 3.5). However, the exergy loss in the ambient air vaporizer (labeled VAP) is not significant (i.e., roughly, 0.1% of real process losses and 1% of ideal process losses). The reason for this becomes more apparent when studying a temperature-exergy plot [3]. The slope on such a plot goes from infinite (i.e., a vertical line) to approximately minus 10 K/(kJ/g) between 300 and 100 K. So, in this temperature range, although there is a significant enthalpy change, there is a minimal change in availability. Note that this is not a real fluid effect, rather it is a consequence of the second law of thermodynamics on the ideal gas behavior of the real fluid [27]. The requirement for the ambient air vaporizer is for the protection of the vacuum pumping system from low temperatures.

4.3 Practical Consideration of Results

At this point, it is important to caution the process engineer in using this information in an actual application. This study has assumed (for the purposes of generality and understanding of process behavior) that the 4.5-K liquefier, compressor and vacuum pumping systems are available in a continuum of capacities. Of course, this is not the case, as these are only available in specific sizes. That being so, this information is intended for the process engineer (rather than the applications engineer) so that process modeling and evaluation may proceed in an informed and efficient manner.

Additionally, the following should be mentioned to clarify this study's intended end objective:

(2) Commercially available vacuum pumping systems require some modifications to compensate for helium's high heat of compression. This involves oil injection modifications not typically supplied or known to the vacuum pump manufacturers, and proper oil cooler sizing. These systems typically consist of a roots (lobe)-blower and either a liquid ring pump or a rotary-vane pump [24].

(3) Commercially available compression systems also require some modifications to compensate for helium's high heat of compression [20, 29]. For present day applications, these systems are typically oil-flooded rotary screw compressors. These compressors have originally been designed for environmental refrigeration, using common refrigerants (such as R-22 or R-134a). As such, although the specific details are very different, the same kind of modifications required for the vacuum

pumping systems are also necessary for the commercial compression systems. Again, many of these modifications are not typically supplied or known by manufacturers.

(4) Although not part of this study, the importance of a proper oil removal system cannot be emphasized enough. This includes bulk oil removal on the vacuum pumping systems and compression systems, as well as oil mist removal (by several stages of coalescers) and oil vapor removal (by activated carbon) [3]. Any fluid impurities (oil vapor, air, etc.) left in the circulating helium will freeze in the 4.5-K and 2-K plants. A proper oil removal system is a relatively simple sub-system to design and fabricate, as compared to the cryogenic and rotating machinery sub-systems, but is quite often inadequately designed (in most present day applications).

(5) Proper mechanical design to minimize the risk of air leaks into the sub-atmospheric process stream(s) is crucial. This includes the use of a guard vacuum, proper helium mass-spectrometer testing during fabrication and proper selection of mechanical joints and seals. In this regard, oil-flooded vacuum pumping and compression equipment serve two purposes in dealing with helium's high heat of compression and sealing. Guard vacuum, as it is known in the field, is a vacuum placed in between an air seal and another sub-atmospheric process stream seal. The guard vacuum is at a lower pressure than the sub-atmospheric process pressure.

(6) A reoccurring theme in all the 2-K system literature review was problems with air leaks. As a matter of practice, such leaks will happen, regardless

of the stringency of testing and robustness of the mechanical design. Therefore, for a practical process design it is prudent to assume that air leaks will be present at some low (ppm) level with occasionally high levels. The practical process design that incorporates continuous purification (i.e., removal of air contamination) will be capable of significantly longer operating periods between complete warm-ups. An integrated helium purifier system, to remove air contamination (from the helium) on the order of 'parts-per-million' (ppm), will greatly extend the 4.5-K plant and 2-K cold box warm-up (to ambient temperature) cycle intervals. A helium purifier is highly desirable in these small 2-K systems, which use warm vacuum pumps that may be required to run for extended periods.

As a constructive example using the results presented, consider the following:

(a) Specified: 2-K load of 174 W

(b) Select configuration C2-A-p.

(c) Select a supply pressure (to the 2-K cold box) of 12 atm.

(d) Select a total heat exchanger size of 40 NTU's

(e) Read from FIGURE 4.1.11; at 40 NTU's, the optimum flow ratio of 77% yields a real COP_{INV} of about 1720 W/W.

(f) Assume (for all cases) the enthalpy difference supplied to the load (i.e., the effective latent heat) is about 20 J/g.

(g) Calculate a total refrigeration flow (from the load, to the VPS) = 174 [W] / 20 [J/g] = 8.7 g/s.

(h) Calculate the required make-up flow from the commercial 4.5-K liquefier system = (1 – 0.77)*8.7 [g/s] = 2.0 g/s.

(i) Calculate the total input power required = 1720 [W/W]*174 [W] / 1000 [W/kW] = 300 kW.

5. CONCLUSIONS

The proposed study goals set forth were achieved, that is;

(1) Three possible 2-K process configurations were identified.

(2) The key process parameters of flow ratio, total heat exchanger NTU's and supply pressure to the 2-K cold box were established.

(3) The influence of these key process parameter choices on the overall performance of the proposed 2-K system configurations was studied.

With this accomplished, a process design basis for a small 2-K refrigeration recovery unit working in conjunction with a commercially available 4.5-K liquefier system, vacuum pumping system and compression system has been established.

In addition, there are a number of important observations to be made from the results previously presented.

(1) An ideal COP_{INV} of about 250 W/W and a real COP_{INV} of about 1800 W/W appears achievable for a 2-K refrigeration-recovery process, operating in conjunction with a small commercially available 4.5-K liquefier system with a 10% Carnot efficiency. This is about 2.8 times less than the ideal COP_{INV} for direct vacuum pumping, and about 3.6 times less than the real COP_{INV} for direct vacuum pumping (without a cold-end heat exchanger), but still 2.0 times greater than the real COP_{INV} for a large efficient 2-K process utilizing cold compressors.

(2) As previously mentioned, for a practical 2-K system it is imperative to incorporate purification to remove air (leak) contamination. In this regard,

configuration C2-A-p lends itself most readily to a simpler integration of flow purification (though not explicitly shown in FIGURE 3.4) as compared to C2-A and C2-B. The latter require separate purification units to process either the full flow or make-up flow to the 4.5-K plant. The process engineer should take heed of a purification capability that is built into the small 4.5-K liquefier systems, as it is typically either inadequate or will seriously reduce the plant capacity during purification. However, in configuration C2-A-p, purification of the *entire* flow stream (rather than just the make-up) is easily accomplished by incorporating carbon beds in the high pressure stream just after the flow leaves the LN boiler (i.e., HX-2 in FIGURE 3.4). Also, by using LN pre-cooling, warm-end heat exchanger (HX-1 in FIGURE 3.4) under-performance (due to flow mal-distribution and/or being under-sized) can be eliminated or greatly reduced in exchange for additional LN consumption. This is an unpublished but extremely common problem in most cryogenic helium systems (that use LN pre-cooling). As can be easily verified, generally, additional LN usage is less costly to the overall process performance than allowing the warm-end heat exchanger under-performance to be carried to below 80 K, thus reducing system capacity.

(3) For configuration C2-B, the blunter ‘knees’ in the curves shown in FIGURES 4.1.3 and 4.1.6 may provide a more stable process for designs with lower total heat exchanger sizes (say, 20 NTU’s and less), despite its greater complexity.

(4) The author acknowledges that the Carnot efficiency used for the LN system and the 4.5-K plant are site/project specific. As such, this analysis can be easily re-performed for site/project specific efficiency values.

(5) The influence of a small variation in the 4.5-K liquefier system Carnot efficiency was shown to have an even smaller influence on the real process overall performance.

In summary, the process performance for handling a 2-K load on the order of 100 W (i.e., about 2 g/s of make-up from the 4.5-K liquefier system) can be significantly increased over direct vacuum pumping by employing one of the process configurations studied. The general advantage of these configurations is in the straightforward integration of these distinct and separate (sub-)systems (i.e., a 2-K cold box and commercially available 4.5-K helium liquefier system, vacuum pumping system and compressor system).

Finally, some recommendations for further study are suggested as follows:

(i) Characterization of isothermal efficiency (with respect to pressure ratio) for various vacuum pumping systems. This would hopefully lead to a classification of pumping systems to use for various flow ranges and methods to improve the efficiency of these systems.

(ii) Testing of alternate heat exchanger designs that are less expensive than brazed-aluminum plate fin heat exchangers but easier to manufacture and have less (sub-atmospheric stream) pressure drop than the spiral-wound finned-tubing ‘pancake’ type [5-8].

REFERENCES

[1] Caillaud, A., Crispel, S., Grabie, V., Delcayre, F., Aigouy, G., "Evolution of the standard helium liquefier and refrigerator range designed by Air Liquide Advanced Technology Division, France," *Proceedings of the 2007 Cryogenic Engineering Conference*, Chattanooga, TN, July 16-20, 2007.

[2] Wilhelm, H.P., Berdais, K.H., Ungricht, T.H., "Improvements of helium liquefaction/refrigeration plants and applications," *Proceedings of the 2007 Cryogenic Engineering Conference*, Chattanooga, TN, July 16-20, 2007.

[3] Ganni, V., *Design of Optimal Helium Refrigeration and Liquefaction Systems*, CEC-ICMC 2007 - CSA Short Course Symposium, 2007.

[4] Peterson, T., "Status: large-scale subatmospheric cryogenic systems," *IEEE 1989 Particle Accelerator Conference*, pp. 1769-1773, 1989.

[5] Collins, S.C., Stuart R.W., Streeter, M.H., "Closed-cycle refrigeration at 1.85 K," *Review of Scientific Instruments*, Vol. 38, No. 11, November 1967, pp. 1654-1657.

[6] Collins, S.C., Streeter, M.H., "Refrigerator for 1.8 K," *Proceedings of the International Cryogenic Engineering Conference*, Vol. 1, 1967, pp. 215-217.

[7] Baldus, W., "Helium-II refrigerator for 300 W at 1.8 K," *Advances in Cryogenic Engineering*, Vol. 16, pp. 163-170, 1971.

[8] Daus, W., Ewald, R., "A refrigeration plant with 300 W capacity at 1.8 K," *Cryogenics*, Vol. 15, pp. 591-598, 1975.

[9] McAshan, M., "Stanford Superfluid Refrigerator," *Fermilab Cryogenic Workshop*, Batavia, IL, June 1980.

[10] Sellmaier, A., Glatthaar, R., Klien, E., "Helium refrigerator with a capacity of 300 W at 1.8 K," *Proceedings of the International Cryogenic Engineering Conference*, Vol. 3, pp. 310-314, 1970.

[11] Steel, A.J., Bruzzi, S., Clarke, M.W., " A 300 W 1.8 K refrigerator and distribution system for the CERN superconducting RF particle accelerator," *Proceedings of the International Cryogenic Engineering Conference*, Vol. 6, pp. 58-61, 1976.

REFERENCES

[12] Adler, E., Chromec, B., Löhlein, K., Purtschert, W., Voigt, T., Gabriel, F., Brunovsky, I., Tucek. L., Quack, H., "Refrigeration at 1.8 K by using a combination of warm screw compressors and cold two-stage turbo-compressors," *Proceedings of the International Cryogenic Engineering Conference*, Vol. 17, pp. 101-108, 1998.

[13] Gistau, G., "The Tore Supra 300 W – 1.75 K refrigerator," *Advances in Cryogenic Engineering*, Vol. 31, pp. 607-615, 1986.

[14] Haberstroh, Ch., "ELBE accelerator: first year of cryogenic operation," *Institut for Energy Engineering Technische Universitat*, Dresden.

[15] Mardion, G.B., Claudet, G., Ferlin, G., Gravil, B., Jager, B., Tavian, L., "Initial operation of the 1.8 K Tore Supra cryogenic system," *Proceedings of the International Cryogenic Engineering Conference*, Vol. 12, pp. 511-518, 1988.

[16] Roussel, P., Girard, A., Jager, B., Rousset, B., Bonnay, P., Millet, F., Gully, P., "The 400 W at 1.8 K test facility at CEA-Grenoble," *Advances in Cryogenic Engineering*, Vol. 51, pp. 1420-1427, 2005.

[17] Grygiel, G., Knopf, U., Lange, R., Peterson, B., Peterson, T., Sellmann, D., Weisend, J., "Status of the TTF cryogenic system," *Advances in Cryogenic Engineering*, Vol. 41, pp. 847-854, 1995.

[18] Horlitz, G., Knopf, U., Lange, R., Peterson, B., Sellmann, D., Trines, D., Peterson, T., "A 1.8 K test facility for superconducting RF cavities," *Advances in Cryogenic Engineering*, Vol. 39, pp. 605-611, 1993.

[19] Strobridge, T.R., Chelton, D.B., "Size and power requirements of 4.2 K refrigerators," *Advances in Cryogenic Engineering*, Vol. 12, pp. 576-584, 1968.

[20] Ganni, V., Knudsen, P., Creel, J., Arenius, D., Casagrande, F., Howell, M., "Screw compressor characteristics for helium refrigeration systems," *Proceedings of the 2007 Cryogenic Engineering Conference*, Chattanooga, TN, July 16-20, 2007.

[21] Grassmann, P., Kopp J., *Kältectechnik*, Vol. 9, 1957, p. 306.

[22] Kays, W.M., London, A.L., *Compact Heat Exchangers* 3rd Ed., Malabar: Krieger Publishing, 1998.

REFERENCES

[23] Perry, R.H., Green, D.W., *Perry's Chemical Engineers' Handbook* 7th Ed., New York: McGraw-Hill, 1997, p. 10-51

[24] O'Hanlon, J.F., *A User's Guide to Vacuum Technology* 2nd Ed., New York: John Wiley and Sons, 1989, pp. 175-178.

[25] Ganni, V., private communication, Hartford screw compressor testing data, August 2006.

[26] Barron, R.F., *Cryogenic Heat Transfer*, Philadelphia: Taylor and Francis, 1999.

[27] Kotas, T.J., *The Exergy Method of Thermal Plant Analysis* 2nd Ed., Malabar: Krieger Publishing, 1985.

[28] Knudsen, P., Ganni, V., "Process study of nominal 2-K refrigeration recovery," *Proceedings of the 2007 Cryogenic Engineering Conference*, Chattanooga, TN, July 16-20, 2007.

[29] Fresco, A., "Optimizing Compressor System Efficiency," *Fermilab Cryogenic Workshop*, Batavia, IL, June 1980.

APPENDIX A

Selected 4.5-K Helium Liquefier Performance Data

	w_L [g/s]	E_L [kW]	P_T [kW]	η_C [-]
GM Cryocooler	0.014	0.0952	19.5	0.5%
Linde 1600	1.97	13.6	124	10.9%
Linde 1600 (Mod)	2.10	14.5	129	11.3%
Linde 2200 (Mod)	3.92	27.1	206	13.2%
CTF (Koch 2200)	5.35	37.0	307	12.0%
CTI/Helix 1500W	11.0	76.0	807	9.4%
SSC ASST-A	34.1	235.9	1582	14.9%

Nomenclature:

w_L - *net helium liquefaction flow [g/s]*

$\Delta\varepsilon_L$ - *specific exergy for 4.5-K liquefaction* = 6.91 [kJ/g]

E_L - *load Carnot (reversible) input power [kW]*, = $w_L * \Delta\varepsilon_L$

w_{LN} - *nitrogen mass flow [g/s]*, 1.3 [gph / (g/s)] *or* 4.9 [ℓph / (g/s)]

η_{LN} - *LN equivalent efficiency [-], = 35% (assumed in this study)*

$\Delta\varepsilon_{LN}$ - *specific exergy for LN cooling*, = 0.70 [kJ/g]

E_{LN} - *LN cooling Carnot input power [kW]*, = $\Delta\varepsilon_{LN} * w_{LN}$

P_{LN} - *equivalent input power for LN [kW]*, = E_{LN} / η_{LN}

P_m – *total input electrical power [kW]*

P_T - *total input power (including LN) [kW]*, = $P_m + P_{LN}$

η_C - *Carnot efficiency*, = E_L / P_T

APPENDIX B

JLab CTF Kinney Vacuum Pump System Isothermal Efficiency Estimate

Description	Symbol	Value	Units	Signal	Notes	Equation
Corrected mass flow	w	9.7	[g/s]		[1], [2]	
Blower suction pressure	$P_{S,b}$	0.025	[atm]	CPI2092	[1]	
Blower suction temperature	$T_{S,b}$	295	[K]	CPI2091	[1]	
Inter-stage pressure	$P_{S,p}$	0.104	[atm]	CPI2093	[1], [3]	
LRP discharge pressure	$P_{D,p}$	1.07	[atm]	CPI284	[1]	
Indicated blower current	I_b	86	[A]	CIT209	[1]	
LRP current	I_p	140	[A]		[4]	
Blower voltage	V_b	386.4	[V]		[5]	
LRP voltage	V_p	480	[V]			
Power factor	ϕ	90%	[-]		[6]	
Total pressure ratio	P_r	42.8	[-]			$= P_{D,p} / P_{S,b}$
Ideal isothermal power	W_{iso}	22.3	[kW]		[7]	$= w * T_{S,b} * (2.0772) * \ln(P_r) / 1000$
Blower actual power input	W_b	51.8	[kW]			$= (1.732) * V_b * I_b * \phi / 1000$
LRP actual power input	W_p	104.8	[kW]			$= (1.732) * V_p * I_p * \phi / 1000$
Isothermal efficiency	η_{iso}	**14.3%**	[-]		[7]	$= W_{iso} / (W_b + W_p)$

Notes:

[1] Data based upon testing conducted at JLab CTF 13-May-2002.
Blower is a Kinney lobe-blower, model KMBD-8000.
Liquid ring pump (LRP) is a Kinney model KLRC-2100S.

[2] Kinney roots-blower operating at 80.5% of 60 Hz.

[3] Inter-stage between blower and LRP.

[4] Based upon curve of LRP current vs. inner stage pressure from Dave Kashy (JLab, 10-Feb-1989).

[5] i.e., 80.5% of 480 V.

[6] Assumed.

[7] Total combined blower & LRP.

APPENDIX C

Data Used for RSC Isothermal Efficiency Characterization

	p_S [atm]	p_D [atm]	p_r [-]	η_i [-]
Sullair - 1st Stage	1.04	2.47	2.375	55.8%
	1.04	3.06	2.942	59.4%
	1.04	3.52	3.385	60.3%
	1.04	4.02	3.865	59.1%
	1.06	4.54	4.283	58.2%
Hartford - LP Inj.	1.00	17.33	17.33	35.7%
	1.00	16.99	16.99	35.4%
	1.00	16.99	16.99	35.6%
	1.00	16.99	16.99	35.8%
	1.00	17.06	17.06	35.0%
Hartford - LP Inj.	1.05	17.33	16.52	36.8%
	1.10	17.33	15.78	37.5%
	1.10	17.33	15.78	37.3%

Nomenclature:

p_S	*suction pressure*
p_D	*discharge pressure*
p_r	*pressure ratio = p_D / p_S*
η_i	*isothermal efficiency*

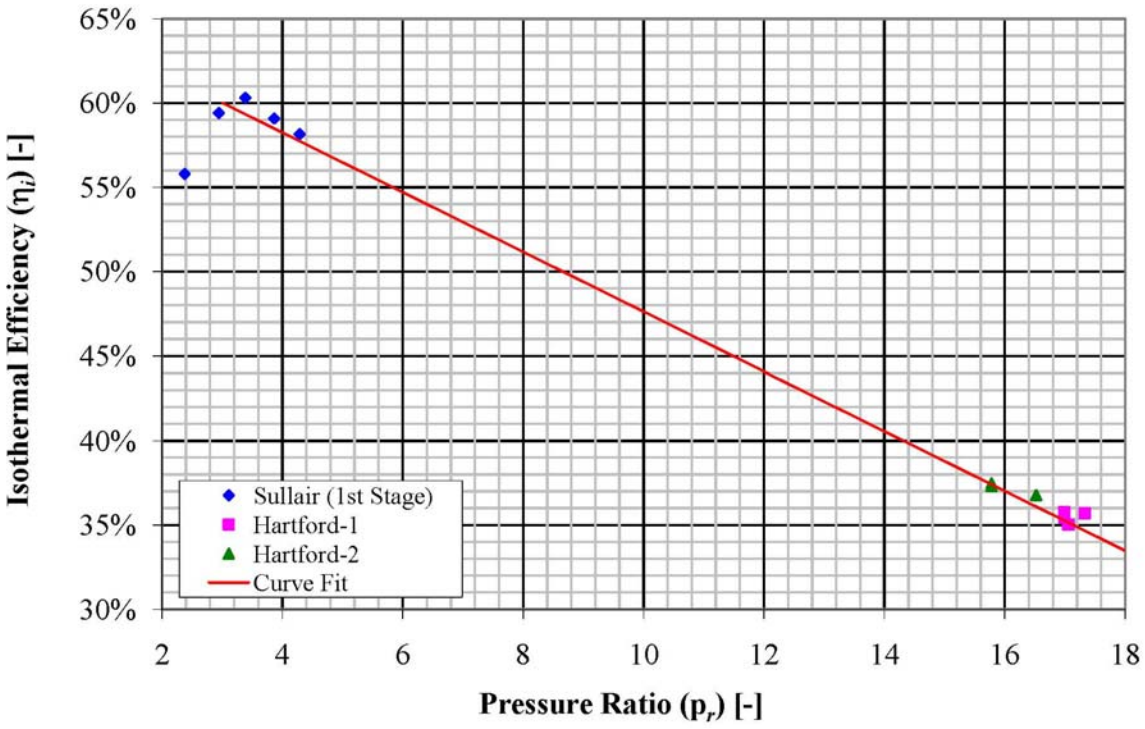

APPENDIX D

Visual Basic Code Outline for Heat Exchanger Cooling Curve Analyses And Process Sheet Calculation Outline

Notes for process sheets:

(i) Yellow background cells are inputs (specified or guessed).

(ii) JT (throttling) valves are assumed to have zero heat leak (i.e., constant enthalpy process).

(iii) Pressure field is completely specified (i.e., simultaneous solution of pressure and temperature fields is not required).

(iv) SS means spread-sheet; VB means visual basic.

C2-A Process Sheet (SS)

- With $T_{l,5}$ specified (i.e., guessed) $T_{h,3}$ calculated from HX performance routine (i.e., outlet temperature calculated based upon inlet conditions, pressure drops, heat in-leak and HX-1 NTU's).
- $h_{h,5}$ calculated using (mixing) energy balance of $h_{h,3}$ and 4.5-K plant enthalpy.
- $h_{h,6}$ calculated using energy balance of HX-2.
- With the above calculated HX-2 NTU's can be calculated.

C2-A Solution Procedure Outline (VB)

- For HX-1 NTU's = 15 to 40 inc. 5
  - Set sub-atm stream HX Δp's and heat in-leak distribution based upon HX NTU's (including vaporizer)
  - For $p_{h,1}$ = 6 to 18 inc. 3 atm.
    - Set $T_{l,5}$ = 3.25, ξ_{hl} = 40%, $\Delta\xi_{hl}$ = 0.01
    - Repeat
      - Repeat
        - Obtain $T_{l,5}$ (calc) – from HX performance routine (i.e., outlet temperature calculated based-upon inlet conditions, pressure drops, heat in-leak and HX-2 NTU's).
        - $T_{l,5}$ (new) = λ* $T_{l,5}$ (calc) + (1-λ)* $T_{l,5}$
      - Iterate until specified tolerance achieved or max. no. iterations exceeded
      - If (calculated) heat load is < 0 then
        - $\xi_{hl} = \xi_{hl} - \Delta\xi_{hl}$
        - $\Delta\xi_{hl} = \alpha * \Delta\xi_{hl}$ (w/ α = 0.1)
      - Else
        - Record solution results
      - $\xi_{hl} = \xi_{hl} + \Delta\xi_{hl}$
    - Iterate until (ξ_{hl} > max) or ($\Delta\xi_{hl}$ < min)

APPENDIX D

C2-A-p Process Sheet (SS)

- Calculate $T_{h,4}$ with $\Delta T_{hN,4}$ specified and $T_{N,3}$ known (i.e., saturated nitrogen vapor).
- Calculate $T_{l,4}$ with $\Delta T_{hl,4}$ specified.
- HX-1 {i.e., HX-1(*h*) and HX-1(*N*)} and HX-2 NTU's can be calculated with the above and specified $\Delta T_{hl,1}$ and $\Delta T_{hN,1}$.
- $h_{h,6}$ calculated using energy balance of HX-3 and specified $h_{l,8}$.
- $h_{h,8}$ calculated using (mixing) energy balance of $h_{h,6}$ and 4.5-K plant enthalpy.
- $h_{h,9}$ calculated using energy balance of HX-4 (i.e., load return enthalpy $h_{l,9}$ is known and $h_{l,8}$ is specified).
- With the above calculated HX-3 and HX-4 NTU's can be calculated.

C2-A-p Solution Procedure Outline (VB)

- For total HX NTU's = 20 to 45 inc. 5
  - For $p_{h,1}$ = 6 to 18 inc. 3 atm.
    - Set $\Delta T_{hl,5}$, $T_{l,8}$ & ξ_{hl} to initial values (they vary w/ $p_{h,1}$)
    - Set $\Delta\xi_{hl} = 0.01$
    - Repeat
      - Call subroutine *Match HX-1 NTU's*
      - If (calculated) heat load > 0 then record solution results
      - $\xi_{hl} = \xi_{hl} - \Delta\xi_{hl}$
    - Iterate until (ξ_{hl} < min) or (error calculating TF)

Subroutine – Match HX-1 NTU's

- If required to match $\Delta T_{hN,1}$ and $\Delta T_{hl,1}$ then
  - Set $\Delta T_{hN,1} = \Delta T_{hl,1}$
  - Call subroutine *Calculate TF* using reduced no. of iterations
  - Repeat
    - Use GoalSeek to set difference between HX-1(h) and HX-1(N) to zero by adjusting $\Delta T_{hN,1}$ and using relaxation parameter.
  - Call subroutine *Calculate TF*
- Iterate until specified tolerance achieved or max. no. iterations exceeded
- Else
  - Call subroutine *Calculate TF*

APPENDIX D

Subroutine – Calculate TF

- Repeat
  - Set HP and sub-atm stream HX Δp's and heat in-leak distribution based upon HX NTU's (including vaporizer)
  - $T_{l,8}$ (calc) – calculated from *HX_Perf* routine (i.e., outlet temperature calculated based-upon inlet conditions, pressure drops, heat in-leak and HX-4 NTU's)
  - Using relaxation, $T_{l,8}$ (new) = λ_2* $T_{l,8}$ (calc) + (1-λ_2)* $T_{l,8}$
  - $T_{l,5}$ (calc) – from *HX_Perf* routine (i.e., outlet temperature calculated based-upon inlet conditions, pressure drops, heat in-leak and HX-4 NTU's)
  - $\Delta T_{hl,5} = T_{h,5} - T_{l,5}$
  - Using relaxation, $\Delta T_{hl,5}$ (new) = λ_1* $\Delta T_{hl,5}$ (calc) + (1-λ_1)* $\Delta T_{hl,5}$
- Iterate until specified tolerance achieved or max. no. iterations exceeded

C2-B Process Sheet (SS)

- $h_{h,7}$ and $h_{hh,7}$ are calculated given $\Delta T_{hl,}7$ (and load temperature $T_{l,7}$).
- If ($h_{h,7} < h_{4K,sup}$) then
  - 4.5-K plant injection between HX-1 and HX-2A
  - $h_{h,7}$ injection between HX-2A and HX-2B
- Else
  - $h_{h,7}$ injection between HX-1 and HX-2A
  - 4.5-K plant injection between HX-2A and HX-2B
- $h_{l,6}$ calculated using energy balance on HX-2B
- $h_{l,4}$ calculated using energy balance on HX-2A/B
- $h_{l,2}$ calculated using energy balance on HX-1
- With all the above calculated, all HX NTU's can be calculated.

C2-B Solution Procedure (VB)

- For total HX NTU's = 20 to 45 inc. 5
  - For $p_{h,1}$ = 6 to 18 inc. 3 atm.
    - Set $\Delta T_{hl,7} = 0.2$, $\Delta\xi_{hl} = 0.01$
    - Repeat
      - Set $\xi_{hl} = 40\%$
      - Call subroutine *Solve for Total No. HX NTU's*
      - If result not OK then
        - $\xi_{hl} = \xi_{hl} - \Delta\xi_{hl}$
        - $\Delta\xi_{hl} = \alpha$* $\Delta\xi_{hl}$ (w/ $\alpha = 0.1$)
      - Else
        - Record solution results
      - $\xi_{hl} = \xi_{hl} + \Delta\xi_{hl}$
    - Iterate until (ξ_{hl} > max) or ($\Delta\xi_{hl}$ < min)

APPENDIX D

Subroutine – Solve for Total No. HX NTU's

- Set sub-atm stream HX Δp's and heat in-leak distribution based upon HX NTU's (including vaporizer).
- Do specified no. of iterations:
  - Use GoalSeek to set difference between set total no. HX NTU's and calculated no. HX NTU's (from sheet) to zero by adjusting $\Delta T_{hl,7}$ and using relaxation parameter.
  - If HX-2 NTU's exceeds set maximum (of 5) then
    - Use GoalSeek to set difference between set HX-2 NTU's and calculated no. HX-2 NTU's (from sheet) to zero by adjusting $\Delta T_{hl,7}$ and using relaxation parameter.
  - Set sub-atm stream HX Δp's and heat in-leak distribution based upon HX NTU's (including vaporizer).

Function HX_T1

Purpose: For HX's with real fluids where the single unknown inlet or outlet temperature of a (multi-stream) HX consists of more than a single stream, the pressures and/or fluids of these (unknown temperature) streams are assumed to be different. As such, they will have different enthalpies so that a direct solution (using an energy balance) is not possible. Rather, an iterative solution is required. By adjusting the unknown temperature to satisfy the HX overall energy balance the solution may be found.

Background:

Objective function (to find zero): $H_T = \sum \dot{m}_i \cdot h_i - H_0 = 0$

Where $\dot{m}_i$ is the mass flow rate (in [g/s]) of stream *i* and all h_i's (enthalpies [J/g] of stream *i*) are a function of a single unknown temperature *T* [K]. The enthalpy flux of all other known temperature HX streams is H_0 [W]. It is important to be consistent with the signs (i.e., flow 'in' vs. 'out').

For Newton's method, the derivative of the objective function is, $\frac{dH_T}{dT} = \sum \dot{m}_i \cdot C_{p,i}$

Where $C_{p,i}$ is the specific heat at constant pressure of stream *i* (in [J/g-K]).

Inputs:

1. For unknown temperature streams:
2. Fluid ID #'s.
3. Mass flow rates, pressures.
4. Initial temperature guess.
5. Enthalpy flux of known temperature HX streams.

Output:

Stream temperature (*T*).

APPENDIX D

Outline:

- Initially use Newton's method but keep track of the sign of the objective function H_T.
- Flag when the solution has been bracketed (i.e., the sign of H_T switches)
- Check to see if solution is converging; i.e.,
  - Abs(H_T) < Abs(old H_T) and,
  - If # iterations ≥ 10 also require (for a converging solution) that the ratio of the fractional tolerance (of T) be L.T. max. allowed.
- If # iterations ≥ 3 and (not converging) then
  - If bounded switch (from Newton's method to) bi-section method
  - Else there is an error.
- Iterate until (exceed max. # iterations) or (fraction tolerance of T < max.)

Note: The motivation for switching from the Newton to bi-section method is to ensure that the solution will converge due to small discontinuities in the fluid enthalpy (as a result of fluid property routine 'curve-fitting'). Also, if the unknown temperature stream is two-phase, this routine will return the quality (since the temperature can be determined from the pressure).

Function HX Anal

Purpose: Calculate the (UA) and NTU's of a real fluid (i.e., non-constant stream capacity) multiple stream (i.e., two or more streams) HX with all 'hot' streams at the same temperature and all 'cold' streams at the same temperature (i.e., two-temperature).

Background:

Consider a sub-division of a real fluid two-temperature multi-stream HX, over which the constant capacity assumption is to be applied:

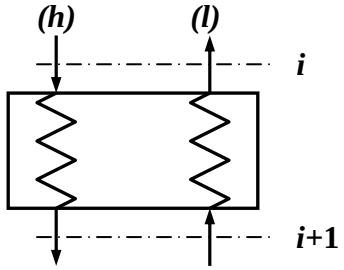

APPENDIX D

$$\Delta h_{h,i} = h_{h,i} - h_{h,i+1} \qquad \Delta h_{l,i} = h_{l,i} - h_{l,i+1}$$

$$q_{h,i} = \dot{m}_h \cdot \Delta h_{h,i} + q_{k,i} \qquad q_{l,i} = \dot{m}_l \cdot \Delta h_{l,i}$$

$$\Delta T_{h,i} = T_{h,i} - T_{h,i+1} \qquad \Delta T_{l,i} = T_{l,i} - T_{l,i+1}$$

$$C_{h,i} = \frac{q_{h,i}}{\Delta T_{h,i}} \qquad C_{l,i} = \frac{q_{l,i}}{\Delta T_{l,i}}$$

$$q_{h,i} = q_{l,i}$$

$$C^*_{R,i} = \frac{C_{l,i}}{C_{h,i}}$$

$$\Delta T_{hl,i} = T_{h,i} - T_{l,i}$$

$$\frac{\Delta T_{hl,i+1}}{\Delta T_{hl,i}} = \theta^*_i$$

$$NTU = \frac{(UA)}{C_{\min}}$$

If $C^*_{R,i} < 1$ then $\ell n\left(\theta^*_i\right) = NTU \cdot \left(1 - C^*_{R,i}\right)$

If $C^*_{R,i} > 1$ then $\ell n\left(\theta^*_i\right) = NTU \cdot \left(\frac{1}{C^*_{R,i}} - 1\right)$

If $C^*_{R,i} = 1$ then $\theta^*_i = 1$ (i.e., a balance HX)

If $C^*_{R,i} = \infty$ then $\ell n\left(\theta^*_i\right) = -NTU$ (i.e., a boiler)

Where,

$C_{h,i}$ or $C_{l,i}$	[W/K]	Stream *(h)* or *(l)* capacity at sub-division *i*
$C^*_{R,i}$	[-]	As defined above
$C_{\min}$	[W/K]	Minimum of $C_{h,i}$ or $C_{l,i}$
$h_{h,i}$ or $h_{l,i}$	[J/g]	Enthalpy of *(h)* or *(l)* stream at sub-division *i*
$\Delta h_{h,i}$ or $\Delta h_{l,i}$		Enthalpy difference of *(h)* or *(l)* stream at sub-division *i*
$\dot{m}_h$ or $\dot{m}_l$	[g/s]	Mass flow rate *(h)* or *(l)* stream
NTU	[-]	Number transfer units, as defined above
$q_{h,i}$ or $q_{l,i}$	[W]	Duty of *(h)* or *(l)* stream at sub-division *i*
$q_{k,i}$	[W]	Heat in-leak at sub-division *i*
$T_{h,i}$ or $T_{l,i}$	[K]	Temperature of *(h)* or *(l)* stream at sub-division *i*
$\Delta T_{h,i}$ or $\Delta T_{l,i}$	[K]	Temperature difference of *(h)* or *(l)* stream at sub-division *i*
$\Delta T_{hl,i}$	[K]	Difference between $T_{h,i}$ and $T_{l,i}$
(UA)	[W/K]	Net thermal rating, as defined above
θ^*_i	[-]	As defined above

APPENDIX D

Note: These equations precisely match the HX overall and sub-division energy balances; also, that $q_{k,i}$ is the heat in-leak (for the sub-division) and is part of the 'hot' stream (h) duty.

Inputs:
1. Number of HX sub-divisions.
2. Number of 'hot' *(h)* streams.
3. Number of 'cold' *(l)* streams.
4. *(h)* stream inlet temperature.
5. *(l)* stream inlet temperature.
6. Either warm-end or cold-end stream temperature difference.
7. Heat in-leak.
8. If it is a boiler.
9. Stream fluid ID #'s, mass flow rates, inlet pressures and pressure drops.

Note: Two type of sub-division 'temperature steps' are allowed; either constant enthalpy (step) or constant enthalpy ratio (step). The 'pressure step' and the heat in-leak distribution will match the temperature step type. Enthalpy is used instead of temperature in order to accommodate the possibility of a phase change.

Output:
Outlet temperatures, total duty, (UA), NTU's.

Outline:
- Solve for unknown temperature (i.e., *(h)* outlet if warm-end temperature difference given and *(l)* outlet if cold-end temperature difference is given).
- Start at HX warm-end and successively solve for *(l)* stream outlet temperature (using routine HX_T1) for each sub-division using the sub-division energy balance and integrating (summing) the duty, (UA) and NTU's.

Function HX Perf

Purpose: There are five different routines associated with HX Perf. For a real fluid two-temperature multi-stream HX, the outlet temperatures are calculated given either (UA), NTU's or thermal effectiveness, or, for the condition of minimum or maximum possible duty.

Background:
The temperature field for the entire HX can be found by solving a system of equations. Namely, the HX sub-division rate equation and the HX sub-division energy balance equation. These are as follows:

APPENDIX D

$$-\theta_i^* \cdot T_{l,i} + \theta_i^* \cdot T_{l,i} + T_{h,i+1} - T_{l,i+1} = 0$$
$$-T_{h,i} + C_{R,i}^* \cdot T_{l,i} + T_{h,i+1} - C_{R,i}^* \cdot T_{l,i+1} = 0$$

Note: Refer to HX Anal for nomenclature and introduction to this background information.

So, for *N* sub-divisions there are a total of $2 \cdot (N+1)$ number of temperatures, 2 of which are known (specified), and there are a total of $2 \cdot N$ number of equations. For a HX with three (3) sub-divisions the system of equations would look as follows:

$$\begin{bmatrix} -\theta_1^* & 1 & -1 & & & \\ C_{R,1}^* & 1 & -C_{R,1}^* & & & \\ & -\theta_2^* & \theta_2^* & 1 & -1 & \\ & -1 & C_{R,2}^* & 1 & -C_{R,2}^* & \\ & & & -\theta_3^* & \theta_3^* & 1 \\ & & & -1 & C_{R,3}^* & 1 \end{bmatrix} \cdot \begin{bmatrix} T_{l,1} \\ T_{h,2} \\ T_{l,2} \\ T_{h,3} \\ T_{l,3} \\ T_{h,4} \end{bmatrix} = \begin{bmatrix} \theta_1^* \cdot T_{h,1} \\ T_{h,1} \\ 0 \\ 0 \\ T_{l,4} \\ C_{R,3}^* \cdot T_{l,4} \end{bmatrix}$$

Of course, this is efficiently solved using a banded matrix solver.

Inputs:

1. HX parameter {i.e., (UA), NTU, effectiveness, max. duty, min. duty}.
2. Value of HX parameter (N/A for max. and min. duty).
3. Number of HX sub-divisions.
4. Number of 'hot' *(h)* streams.
5. Number of 'cold' *(l)* streams.
6. *(h)* stream inlet temperature.
7. *(l)* stream inlet temperature.
8. Heat in-leak.
9. If it is a boiler.
10. Stream fluid ID #'s, mass flow rates, inlet pressures and pressure drops.

Note: Two types of sub-division temperature steps are allowed, either constant enthalpy (step) or constant enthalpy ratio (step). The pressure step and the heat in-leak distribution will match the temperature step type. Enthalpy is used instead of temperature in order to accommodate the possibility of a phase change.

Output:

Outlet temperatures and duty.

APPENDIX D

Outline: *For calculating outlet temperatures given either (UA) or NTU's*

- Set up pressure profile and initial temperature profile (as if the stream capacity were constant).
  - Set up banded matrix.
  - Calculate temperature profile by solving banded matrix.
  - Update temperature field using relaxation technique.
  - Calculate sub-division duties.
  - Determine maximum sub-division duty fractional difference {between *(h)* and *(l)* streams}.
  - Determine maximum fractional difference (change) in temperature field.
  - Iterate until (exceed max. # iterations) or (fraction tolerance < max.)
- Check fractional difference in total duty {between *(h)* and *(l)* streams}.
- If solution did not converge then continue:
- Calculate HX with maximum (and minimum) duty.
- If temperature pinch is on warm-end then use warm-end temperature difference
- Else use cold-end temperature difference.
  - Use the false-position (a bracketing) method (with solution bounds known) with the selected (warm-end or cold-end) temperature difference as the independent variable and the log of the (UA) or NTU's (depending which one was specified as the input) as the dependent variable
  - Iterate until (exceed max. # iterations) or (fraction tolerance < max.)

Outline: *For calculating the outlet temperatures given the effectiveness*

- Calculate HX with maximum (and minimum) duty.
- If temperature pinch is on warm-end then use warm-end temperature difference
- Else use cold-end temperature difference.
  - Use the false-position (a bracketing) method (with solution bounds known) with the selected (warm-end or cold-end) temperature difference as the independent variable and effectiveness as the dependent variable
  - Iterate until (exceed max. # iterations) or (fraction tolerance < max.)

APPENDIX D

Outline: *For calculating the HX with maximum duty*

- Calculate HX with 1 NTU to see whether pinch is on the warm-end or cold-end; whichever end is pinched will be assumed to be the end that is pinched for the maximum duty case (note: it is not really important if it isn't).
- Calculate HX with minimum duty; this provides the upper boundary of the solution bracket.
- To obtain the lower boundary stream temperature difference begin with a stream temperature difference equal to 10 times the max. allowed fractional error
  - Check to see if HX solution (using stream temperature difference) is valid (i.e., results in a solution without a temperature 'cross-over').
  - Check to see if stream temperature difference is less than maximum (i.e., it is 'in-bounds')
  - Increment stream temperature difference by a factor of 10
  - Repeat until there is not a cross-over *and* it is in-bounds
- Now have lower stream difference temperature bound
- Use golden-section technique to find the solution; i.e., iterate until the fractional difference between a solution (no cross-over) and no solution (a cross-over) is acceptably small

Outline: *For calculating the HX with minimum duty*

- Use *HX Anal* to find HX with a duty equal to its heat in-leak

APPENDIX E

Nomenclature and Parameters Used for Process Calculation Sheets

Common Process Configuration Parameters:

$w_{l,1}$	12	[g/s]	*Sub-atmospheric (LP) stream flow rate*
ξ_{hl}		[non-dim.]	*Flow ratio, 40 to 100%*
$p_{h,1}$		[atm]	*Cold box supply pressure, = 6 to 18, inc. 3*
$p_{S,\,RSC}$	1.05	[atm]	*RSC suction and VPS discharge pressure*
p_L	0.031	[atm]	*Load (saturation) pressure*
$T_{h,1}$	300	[K]	*Supply temperature*
$T_{S,\,RSC}$	300	[K]	*RSC suction and VPS discharge temperature*
$T_{l,1}$	300	[K]	*VPS suction temperature*
T_L	2	[K]	*Load (saturation) temperature*
$q_{LK,tot}$	55	[W]	*Total HX heat in-leak*
p_{4K}	3	[atm]	*4.5-K plant supply pressure*
T_{4K}	4.5	[K]	*4.5-K plant supply temperature*
$\eta_{iso,VPS}$	14.5%	[non-dim.]	*VPS isothermal efficiency*
$\eta_{iso,RSC}$		[non-dim.]	*RSC isothermal efficiency,* = 0.6 - 0.0177*($p_{r,c}$ - 3)
$p_{r,c}$		[non-dim.]	*RSC pressure ratio (discharge to suction)*
$\eta_{C,LN2}$	35%	[non-dim.]	*LN system equivalent Carnot efficiency*
$\Delta p_{h,tot}$	0.35	[atm]	*High pressure (HP) stream total pressure drop*
$\Delta p_{l,tot}$		[atm]	*LP stream total pressure drop,* = .0002*Ntu_{tot}
Ntu_{tot}		[non-dim.]	*Total (sum) HX NTU's, = 20 to 45, inc. 5*

Specific Process Configuration Parameters:

Configuration: C1-A

Ntu_{HX-1}	0 to 6	[non-dim.]	*HX-1 NTU's*

Configuration: C2-A

Ntu_{HX-2}	5	[non-dim.]	*HX-2 NTU's*
$\eta_{C,4K}$	10%	[non-dim.]	*4.5-K plant system Carnot efficiency*

Configuration: C2-A-*p*

Ntu_{HX-4}	5	[non-dim.]	*maximum HX-4 NTU's*
$\Delta T_{hl,2}$	40	[K]	*stream (h) to (l) ΔT at T.L. #2*
$\Delta T_{hN,4}$	0.5	[K]	*stream (h) to (N) ΔT at T.L. #4*
$p_{N,3}$	1.2	[atm]	*stream (N) pressure at T.L. #3*
$\Delta p_{N,HX-1}$	0.2	[atm]	*HX-1, stream (N) pressure drop*
$\eta_{C,4K}$	11%	[non-dim.]	*4.5-K plant system Carnot efficiency*

Configuration: C2-B

Ntu_{HX-2}	5	[non-dim.]	*maximum HX-2 NTU's*
$\eta_{C,4K}$	10%	[non-dim.]	*4.5-K plant system Carnot efficiency*

APPENDIX E

Abbreviations:

RSC	*rotary screw compressor system*
VPS	*vacuum pumping system*
4.5-K Plant	*4.5-K plant system (cold box + compressors)*
JT	*Joule-Thompson (throttling) valve*
HX	*heat exchanger*
VAP	*ambient vaporizer*
LOAD	*2-K refrigeration load*
(h), (hh)	*high pressure (HP) streams*
(l)	*sub-atmospheric pressure (LP) stream*
(ll)	*low pressure (LP) streams (>= 1 atm)*
(N)	*nitrogen (liquid and vapor) stream*
T.L. #	*'temperaure level' number*
LN	*liquid nitrogen*

Subscripts (partial list):

C	*Carnot*
c	*compressor*
L	*load*
4K	*4.5-K plant*
LK	*(heat) in-leak*
tot	*total*

Symbols:

w	[g/s]	*mass flow rate*
ξ	[non-dim.]	*mass flow ratio*
p	[atm]	*pressure*
Δp	[atm]	*pressure difference (drop)*
p_r	[non-dim.]	*pressure ratio*
T	[K]	*temperature (absolute)*
ΔT	[K]	*temperature difference*
q	[W]	*duty*
η	[non-dim.]	*efficiency*
COP_{INV}	[W/W]	*inverse of coefficient of performance*

Subscripts:

examples,	$w_{l,1}$	*stream (l) mass flow rate at T.L. #1*
	$\xi_{hl,1}$	*stream (h) to (l) mass flow ratio at T.L. #1*
	$\Delta T_{hl,2}$	*stream (h) to (l) temp. difference at T.L. #2*
	$\Delta p_{N,HX-1}$	*HX-1, stream (N) pressure drop*
	Ntu_{HX-1}	*HX-1 NTU's*

APPENDIX F

Estimate for Increase in 4.5-K Plant Carnot Efficiency for Configuration C2-A-p

		Supply					*Return (or Vent)*				
		ṁ [g/s]	**T** [K]	**p** [atm]	**h** [J/g]	**ε** [kJ/g]	**ṁ** [g/s]	**T** [K]	**p** [atm]	**h** [J/g]	**ε** [kJ/g]
Case 1	**LN Pre-Cooling**	8.46	91.34	4.00	-92.67	6.856	8.46	291.00	1.00	302.06	6.160
Case 2	**LN Pre-Cooling**	0.91	91.34	4.00	-92.67	6.86	0.91	291.00	1.00	302.06	6.16
	He Pre-Cooling (from 2-K Sys.)	2.76	80.00	1.20	431.02	1.031	2.76	288.00	1.05	1511.22	0.032
Case 1 & 2	**4.5-K Helium Liquefaction**	5.73	5.58	3.00	22.74	6.208	3.90	4.46	1.24	30.54	5.493

		Δh [J/g]	**q** [kW]
Case 1	**LN Pre-Cooling**	394.73	3.339
Case 2	**LN Pre-Cooling**	394.73	0.358
	He Pre-Cooling (from 2-K Sys.)	1080.20	2.981
Case 1 & 2	**4.5-K Helium Liquefaction**	7.80	

	Δε [kJ/g]	**B_L** [kW]
	0.695	5.88
	0.695	0.63
	0.999	2.76
	0.715	14.15

Case 1 - Nitrogen Pre-Cooling Only

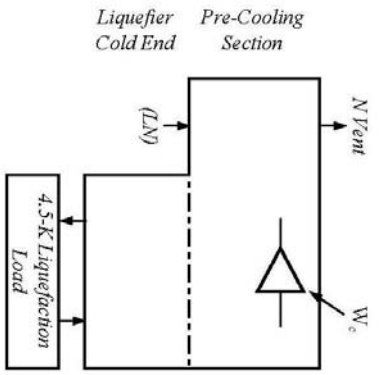

Case 2 - LP Helium Assisting LN Pre-Cooling

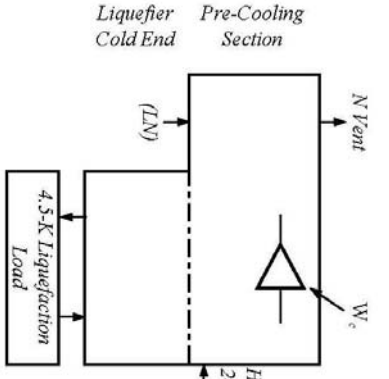

Input power to compressor	W_c	[kW]	**Case 1** 111.3	**Case 2** 111.3	**Ratio**
LN system Carnot efficiency	$\eta_{C,LN}$	[-]	35.0%	35.0%	
LN system exergy	E_{LN}	[-]	5.88	0.63	
Equiv. LN sys. input power	W_{LN}	[kW]	16.8	3.39	$= E_{LN} / \eta_{C,LN}$
Total input power	W_T	[kW]	128.1	114.7	$= W_c + W_{LN}$
4.5-K Liquefier exergy	$E_{L,4K}$	[kW]	14.1	14.1	
System Carnot efficiency	η_C	[-]	11.0%	12.3%	**1.12**

$= E_{L,4K} / W_T$

APPENDIX G

Process Calculation Sheets for Model Configurations at Optimum 'Real' COP_{INV}

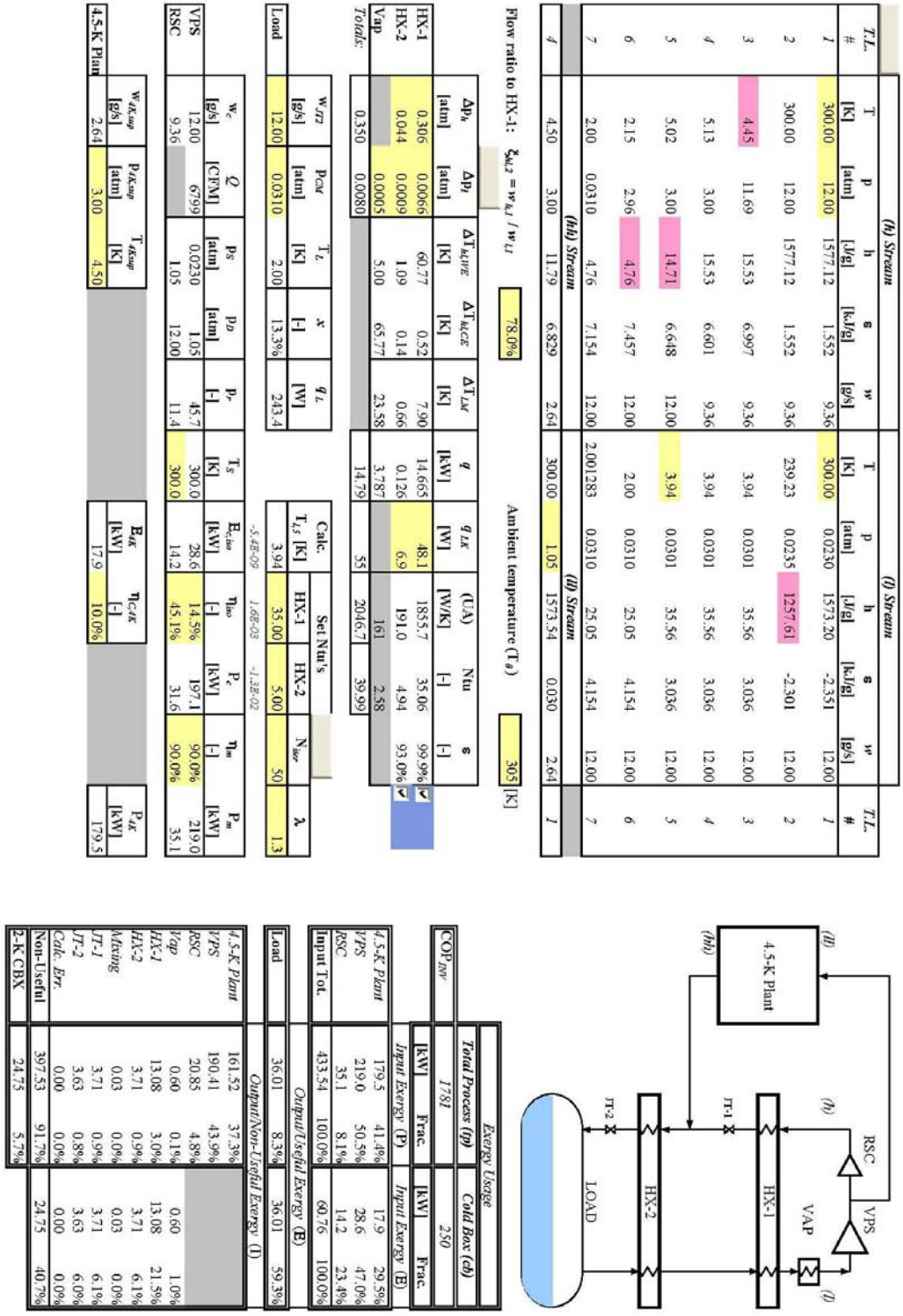

2-K Refrigeration Recovery Process Study — **C2-A**

T.L. #	(h) Stream T [K]	p [atm]	h [J/g]	s [kJ/g]	w [g/s]	(l) Stream T [K]	p [atm]	h [J/g]	s [kJ/g]	w [g/s]	T.L. #
1	300.00	12.00	1577.12	1.552	9.36	300.00	0.0230	1573.20	-2.351	12.00	1
2	300.00	12.00	1577.12	1.552	9.36	239.23	0.0235	1257.61	-2.301	12.00	2
3	4.45	11.69	15.53	6.997	9.36	3.94	0.0301	35.56	3.036	12.00	3
4	5.13	3.00	15.53	6.601	9.36	3.94	0.0301	35.56	3.036	12.00	4
5	5.02	3.00	14.71	6.648	12.00	3.94	0.0301	35.56	3.036	12.00	5
6	2.15	2.96	4.76	7.457	12.00	2.00	0.0310	25.05	4.154	12.00	6
7	2.00	0.0310	4.76	7.154	12.00	2.001283	0.0310	25.05	4.154	12.00	7
	(hh) Stream					(ll) Stream					
4	4.50	3.00	11.79	6.829	2.64	300.00	1.05	1573.54	0.030	2.64	1

Flow ratio to HX-1: $\xi_{hl,2} = w_{hl} / w_{LI}$ = 78.0%

Ambient temperature (T_a) = 305 [K]

	Δp_h [atm]	Δp_l [atm]	ΔT_{hLIVE} [K]	ΔT_{hLCE} [K]	ΔT_{LM} [K]	q [kW]	q_{LK} [W]	(UA) [W/K]	Ntu [-]	ε [-]
HX-1	0.306	0.0066	60.77	0.52	7.90	14.665	48.1	1855.7	35.06	99.9%
HX-2	0.044	0.0009	1.09	0.14	0.66	0.126	6.9	191.0	4.94	93.0%
Vap		0.0005	5.00	65.77	23.58	3.787		161	2.58	
Totals:	0.350	0.0080				14.79	55	2046.7	39.99	

	w_{LT2} [g/s]	p_{CM} [atm]	T_L [K]	x [-]	q_L [W]
Load	12.00	0.0310	2.00	13.3%	243.4

Calc. T_{LS} [K]: 3.94 | -5.45E-09 | 1.68E-03 | -1.38E-02

Set Nu's: HX-1 = 35.00; HX-2 = 5.00

	w_C [g/s]	Q [CFM]	p_S [atm]	p_D [atm]	p_r [-]	T_S [K]	E_{LHX} [kW]	η_{HX} [-]	P_C [kW]	η_M [-]	P_M [kW]
VPS	12.00	6799	0.0230	1.05	45.7	300.0	28.6	14.5%	197.1	90.0%	219.0
RSC	9.36		1.05	12.00	11.4	300.0	14.2	45.1%	31.6	90.0%	35.1

	$w_{LK,sup}$ [g/s]	$p_{LK,sup}$ [atm]	$T_{LK,sup}$ [K]
4.5-K Plant	2.64	3.00	4.50

	E_{LK} [kW]	η_{CLK} [-]
	17.9	10.0%

	P_{LK} [kW]
	179.5

Exergy Usage

COP_INV	Total Process (tp) 1781		Cold Box (cb) 250	
	[kW]	Frac.	[kW]	Frac.
Input Exergy (P)			Input Exergy (E)	
4.5-K Plant	179.5	41.4%	17.9	29.5%
VPS	219.0	50.5%	28.6	47.0%
RSC	35.1	8.1%	14.2	23.4%
Input Tot.	433.54	100.0%	60.76	100.0%
Output/Useful Exergy (E)				
Load	36.01	8.3%	36.01	59.3%
Output/Non-Useful Exergy (I)				
4.5-K Plant	161.52	37.3%		
VPS	190.41	43.9%		
RSC	20.85	4.8%		
Vap	0.60	0.1%	0.60	1.0%
HX-1	13.08	3.0%	13.08	21.5%
HX-2	3.71	0.9%	3.71	6.1%
Mixing	0.03	0.0%	0.03	0.0%
JT-1	3.71	0.9%	3.71	6.1%
JT-2	3.63	0.8%	3.63	6.0%
Calc. Err.	0.00	0.0%	0.00	0.0%
Non-Useful	397.53	91.7%	24.75	40.7%
2-K CBX	24.75	5.7%		

APPENDIX G

2-K Refrigeration Recovery Process Study C2-A-p

T.L. #	(N) Stream T [K]	p [atm]	h [J/g]	ε [kJ/g]	w [g/s]	(h) Stream T [K]	p [atm]	h [J/g]	ε [kJ/g]	w [g/s]	(l) Stream T [K]	p [atm]	h [J/g]	ε [kJ/g]	w [g/s]	T.L. #
1						300.00	12.00	1577.12	1.552	12.00	300.00	0.0237	1573.20	-2.334	12.00	1
2	260.00	1.00	269.80	6.163	4.64	300.00	12.00	1577.12	1.552	12.00	260.00	0.0241	1365.48	-2.308	12.00	2
3	78.89	1.20	77.86	6.370	4.64	91.96	11.94	496.11	2.312	12.00	65.98	0.0253	357.94	-1.148	12.00	3
4	91.34	4.00	-92.67	6.856	4.64	79.39	11.92	430.56	2.474	12.00	65.98	0.0253	357.94	-1.148	12.00	4
	(ll) Stream															
5	79.91	1.20	430.56	1.032	2.76	79.39	11.92	430.56	2.474	9.24	65.98	0.0253	357.94	-1.148	12.00	5
6						4.92	11.69	17.06	6.900	9.24	4.15	0.0301	36.65	2.956	12.00	6
	(hh) Stream					-8.4E-07										
7	4.50	3.00	11.79	6.829	2.76	5.30	3.00	17.06	6.514	9.24	4.15	0.0301	36.65	2.956	12.00	7
8						5.17	3.00	15.85	6.582	12.00	4.15	0.0301	36.65	2.956	12.00	8
9						2.15	2.96	4.82	7.448	12.00	2.00	0.0310	25.05	4.154	12.00	9
10						-9.1E-06 2.00	0.0310	4.82	7.145	12.00	2.00	0.0310	25.05	4.154	12.00	10

Flow ratio to HX-3: $\xi_{hl,5} = w_{h,5} / w_{l,5}$ 77.0%

Ambient temperature (T_0) 305 [K]

HX-2 Needed? TRUE

	Δp_h [atm]	Δp_l [atm]	$\Delta T_{hl,WE}$ [K]	$\Delta T_{hl,CE}$ [K]	ΔT_{LM} [K]	q [kW]	q_{LK} [W]	(UA) [W/K]	Ntu [-]	ε [-]	
HX-1(*h*)	0.056	0.0012	40.00	25.97	32.43	12.090	8.1	372.8	6.41	82.9%	✓
HX-1(*N*)	(N) ▶	0.20	40.00	13.06	25.25	0.890	0.8	35.3	8.24	82.2%	✓
HX-2	0.029		13.06	0.50	3.85	0.791	4.5	205.6	3.26	96.2%	✓
HX-3	0.222	0.0048	13.41	0.78	2.80	3.856	34.8	1378.4	25.41	99.4%	✓
HX-4	0.044	0.0009	1.03	0.15	0.73	0.139	6.9	191.9	4.95	93.2%	✓
Vap		0.0004	5.00	45.00	18.20	2.493		137	2.20		
Totals:	0.350	0.0073				17.77	55.0	2184.0	40.03		

	Set	Error
Set Total Ntu's	40.00	
Set HX-3 Ntu's	25.32	3.5E-03
Set HX-4 Ntu's	5.00	-1.1E-02
Calc. $\Delta T_{hl,5}$ [K]	13.41	1.6E-07
Calc. $T_{l,5}$ [K]	65.98	-3.2E-08
λ (for $\Delta T_{hl,5}$)	0.8	
Calc. $T_{l,8}$ [K]	4.15	-5.9E-06
λ (for $T_{l,8}$)	1.4	
N_{liq}	70	
Max. Error	1.0E-05	

	w_{JT} [g/s]	p [atm]	T [K]	x [-]	q [W]
Load	12.00	0.0310	2.00	13.6%	242.7

Ntu's {HX-1(*h*) - HX-1(*N*)} 1.8E+00 [-]

HX-2 LN_2 quality, x_N 13.3% [-]

HX-1 helium bypass, w_b 0.82 [g/s]

	w_c [g/s]	Q [CFM]	p_S [atm]	p_D [atm]	p_r [-]	T_S [K]	$E_{s,iso}$ [kW]	η_{iso} [-]	P_c [kW]	η_m [-]	P_m [kW]
VPS	12.00	6612	0.0237	1.05	44.4	300.0	28.4	14.5%	195.6	90.0%	217.4
RSC	12.00		1.05	12.00	11.4	300.0	18.3	45.1%	40.5	90.0%	45.0

	w_{sup} [g/s]	p_{sup} [atm]	T_{sup} [K]	E_{sup} [kW]	η_C [-]	W_{sup} [W]	P_{sup} [kW]
LN Sys.	4.64	4.00	91.34	3.21	35.0%		9.18
4.5-K Plan	2.76	3.00	4.50	16.00	11.0%	1156	145.45

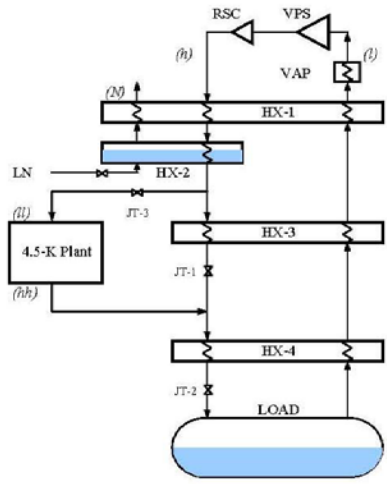

	Exergy Usage: Total Process (tp)		Cold Box (cb)	
COP_{INV}	1718		271	
	[kW]	Frac.	[kW]	Frac.
	Input Exergy (P)		Input Exergy (E)	
4.5-K Plant	145.4	34.9%	16.0	24.3%
LN Sys.	9.2	2.2%	3.2	4.9%
VPS	217.4	52.1%	28.4	43.1%
RSC	45.0	10.8%	18.3	27.7%
Input Tot.	416.99	100.0%	65.84	100.0%
	Output/Useful Exergy (E)			
Load	35.90	8.6%	35.90	54.5%
	Output/Non-Useful Exergy (I)			
4.5-K Plant	129.45	31.0%		
LN Sys.	5.97	1.4%		
VPS	189.01	45.3%		
RSC	26.73	6.4%		
Vap	0.31	0.1%	0.31	0.5%
HX-1	5.75	1.4%	5.75	8.7%
HX-2	0.30	0.1%	0.30	0.5%
HX-3	8.36	2.0%	8.36	12.7%
HX-4	3.97	1.0%	3.97	6.0%
Mixing	0.05	0.0%	0.05	0.1%
JT-1	3.98	1.0%	3.98	6.0%
JT-2	3.57	0.9%	3.57	5.4%
JT-3	3.64	0.9%	3.64	5.5%
Calc. Err.	0.00	0.0%	0.00	0.0%
Non-Useful	381.09	91.4%	29.93	45.5%
2-K CBX	35.90	8.6%		

APPENDIX G

2-K Refrigeration Recovery Process Study C2-B

T.L. #	(h) Stream T [K]	p [atm]	h [J/g]	ε [kJ/g]	w [g/s]	(ii) Stream T [K]	p [atm]	h [J/g]	ε [kJ/g]	w [g/s]	(i) Stream T [K]	p [atm]	h [J/g]	ε [kJ/g]	w [g/s]	T.L. #
1	300.00	12.00	1577.12	1.552	9.48	300.00	1.05	1573.54	0.030	2.52	300.00	0.0230	1573.20	-2.351	12.00	1
2	300.00	12.00	1577.12	1.552	9.48						242.14	0.0235	1272.71	-2.305	12.00	2
3	4.50	11.69	15.67	6.987	9.48						3.84	0.0302	35.05	3.078	12.00	3
						(hh) Stream										
4	4.50	11.69	15.67	6.987	9.48	4.50	3.00	11.79	6.829	2.52	3.84	0.0302	35.05	3.078	12.00	4
5	4.24	11.68	14.87	7.041	9.48	4.24	3.00	10.67	6.904	2.52	3.67	0.0303	34.14	3.151	12.00	5
6	4.24	11.68	14.87	7.041	9.48	4.24	3.00	10.67	6.904	12.00	3.67	0.0303	34.14	3.151	12.00	6
7	2.31	11.65	10.67	7.418	9.48	2.31	2.96	5.32	7.383	12.00	2.00	0.0310	25.05	4.154	12.00	7
8						2.00	0.0310	5.32	7.072	12.00	2.00	0.0310	25.05	4.154	12.00	8

Flow ratio to HX-1: $\xi_{hl,2} = w_{h,1} / w_{l,1}$ 79.0% Ambient temperature (T_0) 305 [K] *Normal Injection ($h_{h,7} <= h_{4K,sup}$)?* TRUE

	Δp_h [atm]	Δp_l [atm]	$\Delta T_{hl,WE}$ [K]	$\Delta T_{hl,CE}$ [K]	ΔT_{LM} [K]	q [kW]	q_{LK} [W]	(UA) [W/K]	Ntu [-]	ε [-]				
HX-1	0.314	0.00675	57.86	0.66	7.73	14.852	49.3	1920.6	35.9	99.9%	☑			
HX-2A	0.004	0.00008	0.66	0.57	0.62	0.011	0.6	17.7	0.4	35.2%	☑			
HX-2B	0.033	0.00070	0.57	0.31	0.56	0.109	5.1	196.1	3.7	85.5%	☑			
Vap		0.00048	5.00	62.86	22.86	3.606		158	2.5		Max. Ntu	N_{iter}	λ	Update Δp's
Totals:	0.350	0.00800				14.97	55.0	2134.4	40.0		40.0	5	1	☑
	0.036	0.00078	◄ (HX-2A + HX-2B) ►			0.12	5.7	213.8	4.1		5.0			

	w_{JT2} [g/s]	p_L [atm]	T_L [K]	x [-]	q_L [W]
Load	12.00	0.0310	2.00	15.7%	236.7

	w_c [g/s]	Q [CFM]	p_S [atm]	p_D [atm]	p_r [-]	T_S [K]	$E_{c,iso}$ [kW]	η_{iso} [-]	P_c [kW]	η_m [-]	P_m [kW]
VPS	12.00	6799	0.0230	1.05	45.7	300.0	28.6	14.5%	197.1	90.0%	219.0
RSC	9.48		1.05	12.00	11.4	300.0	14.4	45.1%	32.0	90.0%	35.5

	$w_{4K,sup}$ [g/s]	$p_{4K,sup}$ [atm]	$T_{4K,sup}$ [K]	$h_{4K,sup}$ [J/g]	$\varepsilon_{4K,sup}$ [kJ/g]	E_{4K} [kW]	$\eta_{C,4K}$ [-]	$P_{inp,4K}$ [W]	P_{4K} [kW]
4.5-K Plan	2.52	3.00	4.50	11.79	6.829	17.1	10.0%	3936	171.3

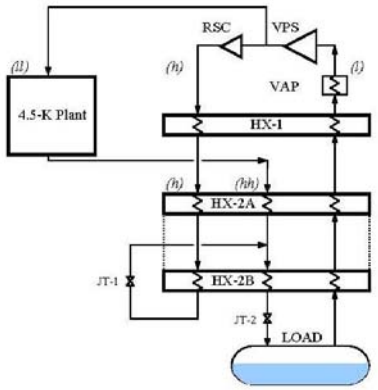

	Exergy Usage: Total Process (tp)		Cold Box (cb)	
COP_{INV}	1799		254.0	
	[kW]	Frac.	[kW]	Frac.
	Input Exergy (P)		Input Exergy (E)	
4.5-K Plant	171.3	40.2%	17.1	28.5%
VPS	219.0	51.4%	28.6	47.5%
RSC	35.5	8.3%	14.4	24.0%
Input Tot.	425.84	100.0%	60.13	100.0%
	Output/Useful Exergy (E)			
Load	35.02	8.2%	35.02	58.2%
	Output/Non-Useful Exergy (I)			
4.5-K Plant	154.18	36.2%		
VPS	190.41	44.7%		
RSC	21.12	5.0%		
Vap	0.55	0.1%	0.55	0.9%
HX-1	13.06	3.1%	13.06	21.7%
HX-2A	0.18	0.0%	0.18	0.3%
HX-2B	2.71	0.6%	2.71	4.5%
JT-1	4.87	1.1%	4.87	8.1%
JT-2	3.73	0.9%	3.73	6.2%
Calc. Err.	0.00	0.0%	0.00	0.0%
Non-Useful	390.82	91.8%	25.11	41.8%
2-K CBX	25.11	5.9%		

VITA

PETER N. KNUDSEN

EDUCATION: **Old Dominion University,** Norfolk, Virginia**,** 2004-2008
M.S. Mechanical Engineering, G.P.A. 4.0

Colorado State University, Fort Collins, Colorado, 1986-1990
B.S. Mechanical Engineering, Graduated Magna Cum Laude, G.P.A. 3.84

EXPERIENCE:

Mechanical Engineer, Cryogenic Systems, *2000 to Present*
Thomas Jefferson National Accelerator Facility (TJNAF), Newport News, Virginia
Presently performing analyses of helium refrigeration process cycles for a 12 GeV planned upgrade at TJNAF, small 2-K helium refrigeration systems and 4.5-K target refrigeration recovery process. Process analyst of 20 K shield refrigerator for James Web Telescope testing at NASA-JSC Space Chamber. Process analyst and lead TJNAF engineer for Brookhaven National Laboratory (BNL) refrigerator upgrade. Cooperatively with BNL, characterized existing plant performance, performed modified plant simulations, developed major component specifications and designed and commissioned new cold boxes. Modifications reduced input power from 9.4 to 5.1 MW, resulting in an operating cost reduction of $50K per week and a one year recovery of capital investment. Responsible for engineering, installation and commissioning of modifications into operating JLab cryogenic systems. Participated in commissioning and performance analysis of SNS compressor system, 4.5-K cold box, and 2-K sub-atmospheric cold compressor system. Lead design engineer for Spallation Neutron Source (SNS) helium cryogenic plant compressor, storage, & purifier systems at Oak Ridge, Tennessee. Supervise and train junior engineers and direct mechanical designers.

Cryogenics and Gases Systems Design Engineer, *1993 to 2000*
NASA at J. F. Kennedy Space Center, Florida
Lead project design engineer and lead piping system design engineer for modifications to a facility, which provides high pressure helium supply to the STS orbiters at the launch pads, to provide a 145 gram per second liquid helium conversion system. Lead thermal cooling, vacuum, and pneumatic systems design engineer for a simulator and related ground support equipment used, in support of the International Space Station, to perform interface functional and verification testing of payload racks prior to being installed in the STS orbiters. Typically responsible for and have participated in many specialized designs of vacuum, pneumatic (nitrogen and helium), water, and cryogenic systems involving fluid flow (single and two-phase, continuum and molecular), heat transfer, and structural analysis. Responsible for the periodic revision of Center engineering standards and component specifications.

Shuttle Fluid Systems Engineer, *1991 to 1993*
NASA at J. F. Kennedy Space Center, Florida
Responsible for the review and development of testing procedures and for the turn-around processing of the auxiliary power units and hydraulic systems of STS orbiters and solid rocket boosters.

PROFESSIONAL & SCHOLARLY ACHIEVEMENTS:

- Received 2007 White House Closing the Circle Award (JLab Cryogenics Group) for Leadership in Federal Environmental Stewardship, Cryogenic Refrigeration System Improvements.
- Received NASA Performance Award, 1993-1994, 1995-1996, 1996-1997, 1997-1998, 1998-1999.
- Received Certificate of Appreciation presented by Kennedy Space Center Director (1998).
- Member of Tau Beta Pi